

Structural Investigation of Anti-*Trypanosoma cruzi* 2-Iminothiazolidin-4-ones Allows the Identification of Agents with Efficacy in Infected Mice

Diogo Rodrigo Magalhaes Moreira,^{*,†,‡} Salvana Priscylla Manso Costa,[‡] Marcelo Zaldini Hernandes,[‡] Marcelo Montenegro Rabello,[‡] Gevanio Bezerra de Oliveira Filho,[‡] Cristiane Moutinho Lagos de Melo,[§] Lucas Ferreira da Rocha,[§] Carlos Alberto de Simone,^{||} Rafaela Salgado Ferreira,⁺ Jordana Rodrigues Barbosa Fradico,⁺ Cássio Santana Meira,[⊥] Elisalva Teixeira Guimarães,^{⊥,#} Rajendra Mohan Srivastava,[†] Valéria Rêgo Alves Pereira,[§] Milena Botelho Pereira Soares,^{⊥,♦} and Ana Cristina Lima Leite[‡]

[†]Departamento de Química Fundamental, Centro de Ciências Exatas and da Natureza, Universidade Federal de Pernambuco, 50670-901, Recife, PE, Brazil

[‡]Departamento de Ciências Farmacêuticas, Centro de Ciências da Saúde, Universidade Federal de Pernambuco, 50740-520, Recife, PE, Brazil

[§]Centro de Pesquisas Aggeu Magalhaes, Fundação Oswaldo Cruz, CEP, 50670-420, Salvador-PE, Brazil

^{||}Departamento de Física and Informática, Instituto de Física, Universidade de São Paulo, CEP 13560-970, São Carlos, SP, Brazil

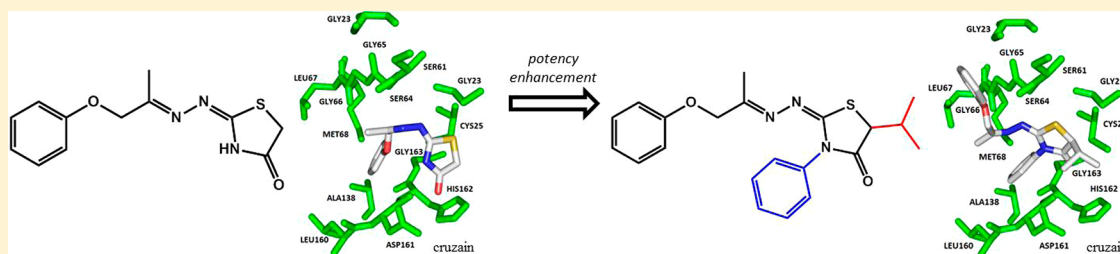
⁺Departamento de Bioquímica and Imunologia, Universidade Federal de Minas Gerais, CEP 31270-901, Belo Horizonte, MG, Brazil

[#]Departamento de Ciências da Vida, Universidade Estadual da Bahia, CEP 41150-000, Salvador, BA, Brazil

[⊥]Centro de Pesquisas Gonçalo Moniz, Fundação Oswaldo Cruz, CEP 40296-710, Salvador, BA, Brazil

[♦]Centro de Biotecnologia and Terapia Celular, Hospital São Rafael, CEP 41253-190, Salvador, BA, Brazil

S Supporting Information



ABSTRACT: We modified the thiazolidinic ring at positions N3, C4, and C5, yielding compounds 6–24. Compounds with a phenyl at position N3, 15–19, 22–24, exhibited better inhibitory properties for cruzain and against the parasite than 2-iminothiazolidin-4-one 5. We were able to identify one high-efficacy trypanocidal compound, 2-minothiazolidin-4-one 18, which inhibited the activity of cruzain and the proliferation of epimastigotes and was cidal for trypomastigotes but was not toxic for splenocytes. Having located some of the structural determinants of the trypanocidal properties, we subsequently wished to determine if the exchange of the thiazolidine for a thiazole ring leaves the functional properties unaffected. We therefore tested thiazoles 26–45 and observed that they did not inhibit cruzain, but they exhibited trypanocidal effects. Parasite development was severely impaired when treated with 18, thus reinforcing the notion that this class of heterocycles can lead to useful cidal agents for Chagas disease.

INTRODUCTION

The World Health Organization estimates that 5–10% of Latin America's population is afflicted by Chagas disease, which is caused by the protozoan *Trypanosoma cruzi*.¹ Current treatment is solely based on benznidazole (Bdz), a nitroimidazole compound. Bdz is cidal for bloodstream trypomastigotes and thus efficient in eliminating parasite in circulation during the initial stages of infection (acute and asymptomatic chronic).^{2,3} The efficacy of Bdz for patients with Chagas-related cardiomyopathy is still unknown,

although a clinical trial (BENEFIT) aiming to investigate this is expected to be concluded in 2013.^{4,5} However, many patients experience drug intolerance and adverse effects for Bdz.⁶ Thus, there is a need to look for other drugs to treat Chagas disease.

A useful strategy for anti-*T. cruzi* drug design is to inhibit the cysteine protease cruzain. Most of the functional properties of

Received: July 25, 2012

Published: November 20, 2012

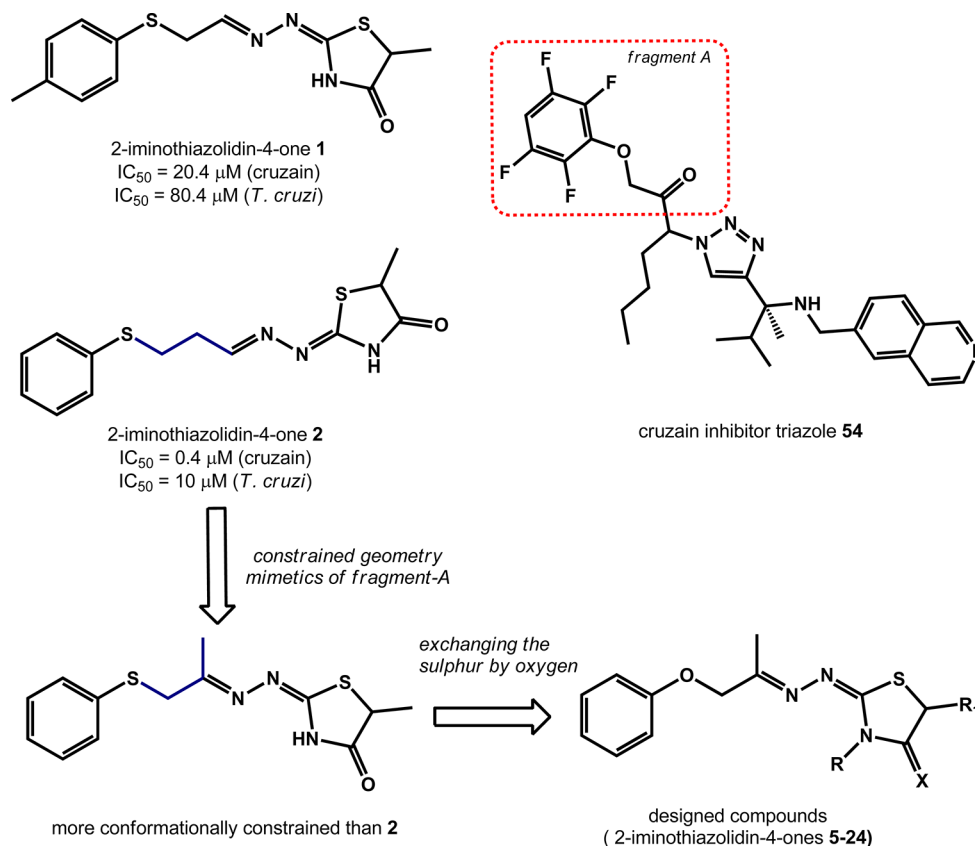


Figure 1. Structural design of new 2-iminothiazolidin-4-ones as trypanocidal agents.

cruzain have been revealed in the recent years.^{7–12} For example, cruzain prevents macrophage activation, probably by degrading macrophage proteins such as the nuclear factor NF- κ B. Cruzain-deficient *T. cruzi* is viable but unable to invade host cells.⁹ On the other hand, cruzain protects infected cardiomyocytes from apoptosis, which is essential for a pathogenic outcome.¹⁰ Cruzain is also responsible for the proteolytic cleavage of kinins that, once released, trigger bradykinin receptors. These receptors in cooperation with endothelin receptors are involved in vascular permeability, which is beneficial for parasite invasion and its persistence in the tissue.^{11,12} Given these functional properties, cruzain is a valid *T. cruzi* drug target.

Since the discovery that thiosemicarbazones are cruzain inhibitors,^{13–16} many attempts have been made to explore the structure–activity relationships (SAR) with a view to designing compounds with improved trypanocidal effects.^{17–21} Recently, potent triazole-based inhibitors that covalently entrap cruzain have been identified. The triazole family of inhibitors bind to the amino acid CYS25 and establish polar interactions with amino acids GLY66 and GLN19 in this binding pocket to stabilize the cruzain–ligand complex.^{22,23} Similar interactions have been observed for other cruzain inhibitors.²⁴ Some variants of this family of triazole inhibitors are cidal for the parasite. One good example is the aryloxymethyl ketone triazole **54**, which eradicates blood parasitemia when administered to *T. cruzi*-infected mice intraperitoneally at 20 mg/kg.²³ The results support the feasibility of employing multiple tactics to inhibit cruzain, which is essential for *T. cruzi* infection.

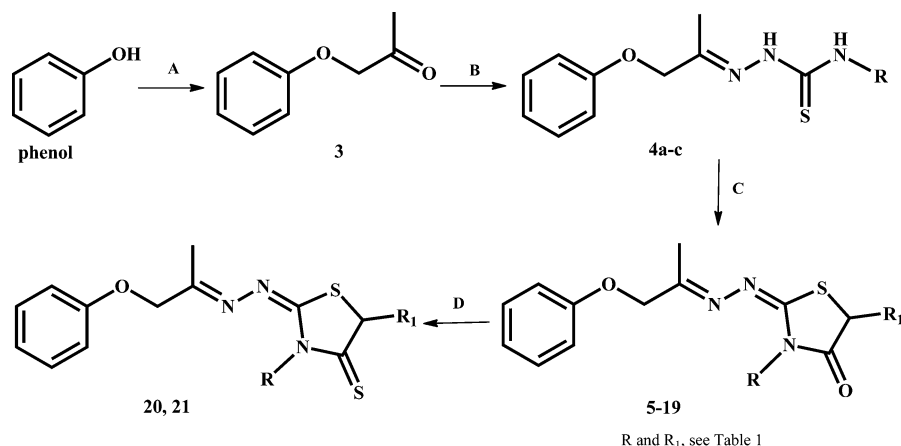
We selected 2-iminothiazolidin-4-ones for development as trypanocidal compounds because of their structural similarity to cruzain-inhibiting thiosemicarbazones. The most potent 2-iminothiazolidin-4-ones we had previously identified were

equipotent to Bdz but less potent than their thiosemicarbazone analogues for cruzain and parasite inhibition assays. However, we also observed that 2-iminothiazolidin-4-ones had low toxicity for mammalian cells (mouse splenocytes), a feature not generally observed in thiosemicarbazones.^{25–27}

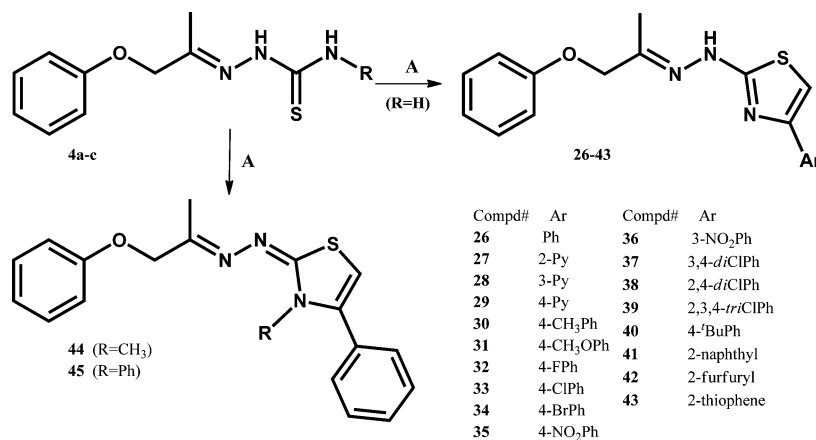
For the design of new anti-*T. cruzi* 2-iminothiazolidin-4-ones, we combined some chemical features of cruzain inhibitor **54** and of our previously tested 2-iminothiazolidin-4-ones (compounds **1** and **2**, Figure 1). All these newly designed 2-iminothiazolidin-4-ones share an aryloxypropylimine group. This was introduced because of the similarity, in terms of geometry and flexibility, to the aryloxymethyl ketone group of the cruzain inhibitor **54**. Our previous model for the docking of 2-iminothiazolidin-4-ones with cruzain suggests that the thiazolidinic ring establishes both polar and hydrophobic interactions with cruzain. As a way of locating the structural determinants of cruzain affinity, we derived a series of 2-iminothiazolidin-4-ones **5–24** by varying substituents around the thiazolidinic ring at positions N3, C4, and C5. Bearing in mind the bioisosteric relationship between 2-imino-1,3-thiazoles and 2-iminothiazolidin-4-ones,²⁸ we prepared the 2-imino-1,3-thiazoles **26–45**. Therefore, we synthesized 2-iminothiazolidin-4-ones **5–19**, their analogues 2-iminothiazolidin-4-thiones **20** and **21**, and 2-imino-1,3-thiazoles **26–45** and evaluated their activity against cruzain and the parasite.

RESULTS

Chemistry. The thiosemicarbazones **4a–c** were prepared by reacting commercially available phenoxy-2-propanone **1** with the appropriate thiosemicarbazide in an ultrasound bath in the presence of catalytic AcOH. 2-Iminothiazolidin-4-ones **5–19**

Scheme 1. Synthetic Procedures for 2-Iminothiazolidin-4-ones 5-19 and 2-Iminothiazolidin-4-thiones 20, 21^a

^aReagents and conditions: (A) 2-chloroacetone, K₂CO₃, butanone, ultrasound bath, rt, 2 h, yield of 68% (B) thiosemicarbazides, EtOH, AcOH, ultrasound bath, rt, 30 min, yields of 65–82%; (C) ethyl 2-bromoacetate or ethyl 2-substituted-2-bromoacetates; NaOAc, EtOH, reflux, overnight, yields of 38–84%; (D) Lawesson's reagent, 1,4-dioxane/toluene, reflux, 20 h, yields of 54% (20) and 60% (21).

Scheme 2. General Synthetic Procedures for 2-Imino-1,3-thiazoles 26–45^a

^aReagents and conditions: (A) substituted 2-bromoacetophenones, 2-propanol, ultrasound irradiation, rt, 30–60 min, yields of 48–85%.

were prepared by reacting the respective thiosemicarbazones **4a–c** with commercially available ethyl 2-bromoacetate or preparing the desired 2-substituted-2-bromoacetates. These reactions were carried out in the presence of an excess of anhydrous NaOAc under reflux, affording compounds **5–19** in acceptable yields (38–84%). For the conversion of 2-iminothiazolidin-4-ones **7** and **19** into 2-iminothiazolidin-4-thiones **20** and **21**, we used Lawesson's reagent as the thionation reagent (yields of 54% and 60%, respectively) (Scheme 1). 2-Imino-1,3-thiazoles **26–45** were prepared via a Hantzsch synthesis between thiosemicarbazones **4a–c** and substituted 2-bromoacetophenones (Scheme 2). These reactions proceed well upon refluxing with ethanol (1–3 h), but we adapted them under ultrasound conditions²⁹ using propanol as a solvent³⁰ and observed excellent yields in general (48–85%) and shorter times (30 min in most cases).

We attempted to define the relative configuration of the iminic bond. Chemical shifts in the methyl and methylene of the aryloxypropylimine group were diagnostically useful for identifying an *E*-isomer (for details, see the Experimental Section). Moreover, we succeeded in crystallizing the 2-iminothiazolidin-4-one **12** and the thiosemicarbazones **4a** and **4c** suitable for X-ray analysis. High-performance chromatography revealed a

mixture of isomers (9.5/0.5) for thiosemicarbazones **4a** and **4c**, and the major isomer has an *E*-geometry. On the other hand, chromatographic analysis in practice revealed only one major isomer for compounds **5–24** and **26–45**. 2-Iminothiazolidin-4-one **12** has an *E*-geometry (Figure 2). It is therefore highly probable that all 2-iminothiazolidin-4-ones **5–24** as well as 2-imino-1,3-thiazoles **26–45** have the same *E*-geometry. For compounds **5–9**, an important structural assignment is the location of an iminic bond in C2. X-ray analysis and quantum chemistry calculations for other 2-iminothiazolidin-4-ones structurally related to compounds **5–9** had suggested that the iminic bond is exocyclic in relation to heterocyclic ring (Figure S1, Supporting Information). It would, therefore, seem fair to suggest that the structures proposed for **5–9** are the correct ones.

Structure–Activity Relationships (SAR). We first assayed the viability of BALB/c mouse splenocytes treated with 2-iminothiazolidin-4-ones **5–19** and **22–24**, 2-iminothiazolidin-4-thiones **20** and **21**, or 2-imino-1,3-thiazoles **26–45**. Once the toxicity to mammalian cells had been determined, we focused on evaluating their effects in *T. cruzi* in vitro assays. We tested against epimastigotes (axenic culture) and bloodstream trypomastigotes of the Y strain (Tables 1, 2, and 4). Compounds that showed IC₅₀ values comparable to benznidazole (Bdz) or

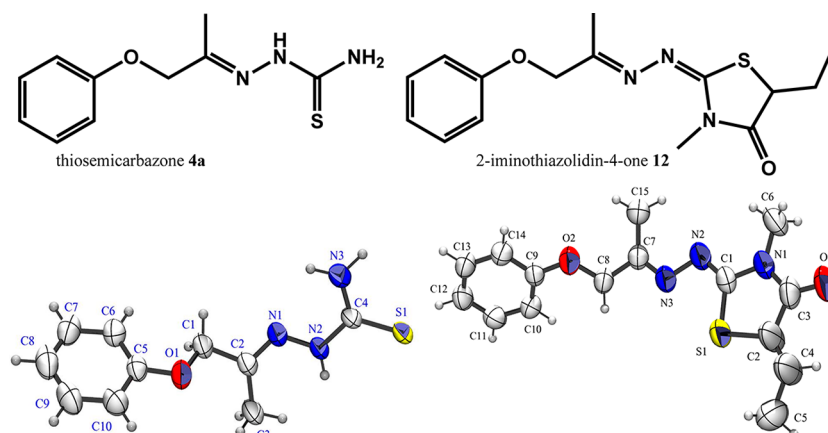


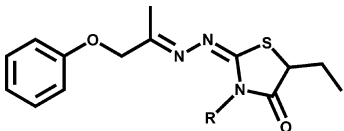
Figure 2. Structures of compounds 4a and 12 determined by X-ray analysis. Anisotropic thermal ellipsoids are drawn at a 50% level. For details, see the Experimental Section and Supporting Information.

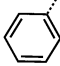
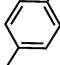
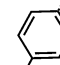
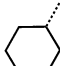
Table 1. Anti-*T. cruzi* Activities of 2-Iminothiazolidin-4-ones 5-19 and 2-Iminothiazolidin-4-thiones 20, 21

Cpd	R ₁	Y strain <i>T. cruzi</i> IC ₅₀ (μM)		toxicity to splenocytes μg/mL (μM) ^[c]
		trypomastigotes ^[a]	epimastigotes ^[b]	
5	H	19.0	23.2	>100 (380)
6	CH ₃	ND	ND	>100
7	C ₂ H ₅	ND	ND	>100
8	CH(CH ₃) ₂	16.8	12.2	>100
9	Ph	18.7	34.8	25
10	H	ND	ND	>100
11	CH ₃	ND	ND	25
12	C ₂ H ₅	ND	ND	>100
13	CH(CH ₃) ₂	10.7	14.0	>100 (313)
14	Ph	18.0	12.0	>100 (283)
15	H	18.0	25.8	>100
16	CH ₃	29.0	31.8	100
17	C ₂ H ₅	5.8	11.1	100 (272)
18	CH(CH ₃) ₂	6.1	4.9	>100 (262)
19	Ph	11.1	15.6	>100 (240)
20	Ph/Ph	11.2	4.2	100 (231)
21	H / C ₂ H ₅	31.5	26.1	25 (81)
Bdz	-	6.2	6.6	25 (96)
Nfx	-	2.7	1.9	1.0
SAP	-	-	-	<1.0

^aDetermined 24 h after incubation of trypomastigotes with the compounds. ^bDetermined 11 days after incubation of epimastigotes with the compounds. IC₅₀ was calculated from at least five concentrations using concentrations in triplicate (SD ± 10%). ^cHighest nontoxic concentration for mouse splenocytes after 24 h of incubation in the presence of the compounds. Bdz: benznidazole; Nfx: nifurtimox; Sap: saponin.

Table 2. Modification of the 2-Iminothiazolidin-4-one 17 toward Compounds 22–24^a



Cpd	R	Y strain <i>T. cruzi</i> IC ₅₀ (μM)		toxicity to splenocytes μg/mL (μM) ^[c]
		Trypomastigotes ^[a]	epimastigotes ^[b]	
17		5.8	11.1	100 (272)
22		19.9	15.0	100 (262)
23		9.0	6.8	100 (251)
24		ND ^[d]	ND	>100 (268)

^aSee footnote in Table 1. ND, not determined.

nifurtimox (Nfx) were further selected for assays of in vitro infection of host cells. The inhibitory activity against cruzain was measured based on the cleavage of the substrate Z-FR-AMC.³¹ Compounds were first tested at 20 or 100 μM, and a dose–response curve was determined and the IC₅₀ calculated for the

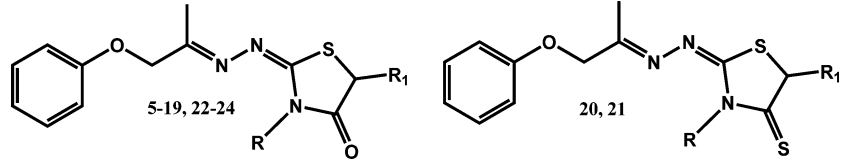
most active compounds. We also evaluated the compounds against the mammalian proteases cathepsins L and S (Tables 3 and 4).

Of all the tested compounds, 2-iminothiazolidin-4-one 18 possessed the highest overall trypanocidal potency, with IC₅₀ values of 6.1 and 4.9 μM for bloodstream trypomastigotes and axenic epimastigotes of the Y strain, respectively (Table 1). It also had trypanocidal properties comparable to those of BdZ. However, 2-iminothiazolidin-4-one 18 does not affect the cell viability of mouse splenocytes even at concentrations of up to 100 μg/mL (262 μM).

The SAR study which led to the identification of 2-iminothiazolidin-4-one 18 began with two kinds of modifications of the thiazolidinic ring: (a) variation of the substituents at C5; (b) replacement of NH with *N*-methyl and *N*-phenyl. These modifications yielded 2-iminothiazolidin-4-ones 5–19. For cruzain inhibition, we observed that modifications at N3 affect cruzain inhibition more than those at C5. For example, most compounds with a free NH (5–9) or an *N*-methyl (10–14) did not inhibit cruzain, while compounds with an *N*-phenyl (15–19) did (Table 3). For *T. cruzi*, we observed somewhat similar behavior, except for compounds 5, 8, and 13 which displayed good trypanocidal properties. In general, *N*-phenyl compounds 15–19 were potent trypanocidal agents.

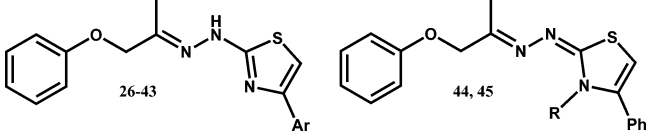
We observed interesting SAR when different substituents were attached at C5 in 2-iminothiazolidin-4-ones 15–19. Inserting a methyl (16), ethyl (17), or isopropyl (18) at position C5 did not increase the affinity for cruzain when compared to the nonsubstituted 2-iminothiazolidin-4-one 15; all of them had

Table 3. Protease Inhibition



compd	<i>T. cruzi</i> cruzain ^a		cathepsin L (% inhibition at 100 μM) ^b	IC ₅₀ μM (SD)	
	% inhibition at 20 μM	IC ₅₀ , μM		cathepsin L	cathepsin S
5	0 ± 2		1 ± 1.5	>100	>100
6	3		0		NT
7	5		5		ND
8	60.8	18.9 ± 0.9	11 ± 2		ND
9	63 ± 2	ND ^d	NT		NT
10	0		NT		NT
11	0		NT		NT
12	50	31.9 ± 1.0	6	>100	>100
13	81	8.0 ± 0.1	0 ± 2	>100	>100
14	27 ± 4	ND ^d	NT		NT
15	66	10.2 ± 0.5	0	>100	>100
16	50	10.8 ± 1.0	0		NT
17	66 (64) ^c	9.5 ± 0.07	4 ± 1	>100	>100
18	78 (81) ^c	6.6 ± 0.05	10 ± 4	>100	>100
19	43 ± 2	ND ^d	15 ± 2		NT
20	72 ± 5.0 (79) ^c	7.0 ± 0.4	89 ± 5	10.8 ± 0.7	NT
21	48 ± 1.0	18.7 ± 2.0	81 ± 6	13.8 ± 2.0	NT
22	65	11.8 ± 0.5	NT		NT
23	71	8.7 ± 0.1	NT		NT
24	10 ± 2		NT		NT

^aAfter 10 min of preincubation with the inhibitor before adding the fluorescent cruzain substrate Z-FR-AMC. ^bAfter 45 min of incubation before adding the fluorescent cathepsin substrate Z-FR-pNA. Percentage of inhibition is the average of triplicate runs determined in one experiment. IC₅₀ was calculated from at least seven concentrations. ^cIn parentheses, experiments using 0.01% of Triton X-100 in the reaction buffer. ^dNot determined because of the low solubility in 0.1 M sodium acetate pH 5.5. NT is not tested.

Table 4. Cruzain and Anti-*T. cruzi* Activities of 2-Imino-1,3-thiazoles 26–45


compd	Ar/R	% of cruzain inhibition at 20 μM^a	Y strain <i>T. cruzi</i> , IC ₅₀ (μM)		toxicity splenocytes $\mu\text{g/mL}$ (μM) ^d
			trypomastigotes ^b	epimastigotes ^c	
26	Ph	no inhib	19.6	ND	50 (154)
27	2-Py	no inhib	34.8	11.8	100 (308)
28	3-Py	no inhib	12.3	20.5	100 (308)
29	4-Py	13.3 \pm 3.8 ^e	3.9	4.0	100 (308)
30	4-CH ₃ Ph	no inhib	49.7	67.0	100 (296)
31	4-CH ₃ OPh	no inhib	17.8	14.9	100 (283)
32	4-FPh	no inhib	11.5	41.3	>100 (293)
33	4-ClPh	13 \pm 6	ND	57.1	100 (280)
34	4-BrPh	25 \pm 1	ND	49.8	100 (249)
35	4-NO ₂ Ph	no inhib	5.7	1.9	100 (271)
36	3-NO ₂ Ph	no inhib	3.8	4.0	100 (271)
37	3,4-diClPh	20 \pm 6	17.0	19.0	25 (63.9)
38	2,4-diClPh	40 \pm 6	17.0	42.2	<1 (2.8)
39	2,3,4-triClPh	no inhib	ND	ND	>1 (2.3)
40	4 ^t BuPh	no inhib	ND	ND	50 (131)
41	β Naph	no inhib	36.4	83.0	>100 (268)
42	2-furfuryl	4.7 \pm 3.2 ^e	17.7	26.6	>100 (319)
43	2-thiophene	30 \pm 6 ^e	37.6	16.6	50 (128)
44	CH ₃	no inhib	174.7	25.6	10 (29.5)
45	Ph	no inhib	61.1	2.6	>100 (250)

^aAfter 10 min of preincubation with the inhibitor before adding the fluorescent protease substrate Z-FR-AMC. ^bDetermined 24 h after incubation of trypomastigotes with the compounds. ^cDetermined 11 days after incubation of epimastigotes with the compounds. IC₅₀ was calculated from at least five concentrations using concentrations in triplicate (SD \pm 10%). ^dHighest nontoxic concentration for mouse splenocytes after 24 h of incubation in the presence of the compounds. ^eCompounds tested at 100 μM . no inhib mean no cruzain inhibition was observed.

the same range of IC₅₀s. However, varying substituents at C5 resulted in different trypanocidal compounds. For example, ethyl (17), and isopropyl (18) compounds were 4-times more potent than compound 15. 2-Iminothiazolidin-4-ones 17 and 18 have an IC₅₀ of 5.8 and 6.1 μM for trypomastigotes, which is equal in potency to Bdz (IC₅₀ of 6.1 μM) and roughly half as potent as Nfx (IC₅₀ of 2.7 μM). Of the five *N*-phenyl 2-iminothiazolidin-4-ones 15–19, only the compound which has a phenyl at C5 (19) showed low inhibitory properties for cruzain but exhibited trypanocidal effects.

Given these promising results, we next wanted to determine whether the conversion of 2-iminothiazolidin-4-ones into 2-iminothiazolidin-4-thiones leads to enhanced potency. We selected 2-iminothiazolidin-4-ones 12 (inactive as trypanocidal and cruzain inhibitor) and 19 (a potent trypanocidal and weak inhibitor of cruzain) to convert into their respective thione variants (Tables 1 and 3). The data revealed that attaching a thionyl at C4 improves cruzain affinity. 2-Iminothiazolidin-4-one 12 did not inhibit cruzain at 20 μM , while 2-iminothiazolidin-4-thione 21 had an IC₅₀ of 18.7 \pm 2.0 μM . This was even more pronounced when we compared 2-iminothiazolidin-4-thione 20 with 2-iminothiazolidin-4-one 19. Compound 20 exhibited an IC₅₀ of 7.0 \pm 0.4 μM for cruzain, while compound 19 had an IC₅₀ > 20 μM . In relation to *T. cruzi*, 21 showed low trypanocidal activity while its counterpart 12 was inactive and compounds 19 and 20 were almost equipotent. In general, replacing a carbonyl with thiocarbonyl enhances the inhibitory properties of 2-iminothiazolidin-4-ones against cruzain, but it does not

necessarily lead to a significant enhancement of potency against the parasite.

Of the compounds described in Table 1, the phenyl group in N3 was identified as the best substituent for conferring anti-*T. cruzi* and cruzain inhibition properties, along with an ethyl or isopropyl attached to C5. We aimed to enhance potency by preparing 17 analogues. To this end, we attached other substituents to N3. We succeeded in preparing 2-iminothiazolidin-4-ones 22, 23, and 24 (Table 2). Replacing an *N*-phenyl (17) with *N*-cyclohexyl (24) was deleterious for cruzain affinity and for anti-*T. cruzi* activity, while replacing it with *N*-tolyl (22) or *N*-(4-methoxyphenyl) (23) retains cruzain affinity. Similar to *N*-phenyl 17, variants 22 and 23 were toxic for trypomastigotes.

The inhibitory property of 2-iminothiazolidin-4-ones 5–24 for cruzain is centered on the key role of the thiazolidinic ring. We decided to explore the thiazolidine–thiazole isosterism. To this end, a congener series of 2-imino-1,3-thiazoles 26–45 was prepared, covering a variety of substitutions at position C4. However, none of the thiazoles inhibited cruzain activity (Table 4). 2-Iminothiazolidin-4-ones and 2-imino-1,3-thiazoles can be viewed as potential bioisosteric heterocycles,²⁸ but this did not prove to be the case, at least not in terms of cruzain inhibition. We first thought the lack of cruzain inhibition for thiazoles 26–45 was merely due to the presence of an aromatic ring at C4. However 2-iminothiazolidin-4-ones 9 and 19 bear a phenyl group at C5, and they still have some activity against cruzain (Figure 3). It seems that the cruzain binding site requires stereo- and electronic-specificity. Nonetheless, 2-imino-1,3-thiazoles 26–45 have a broad range of trypanocidal properties.

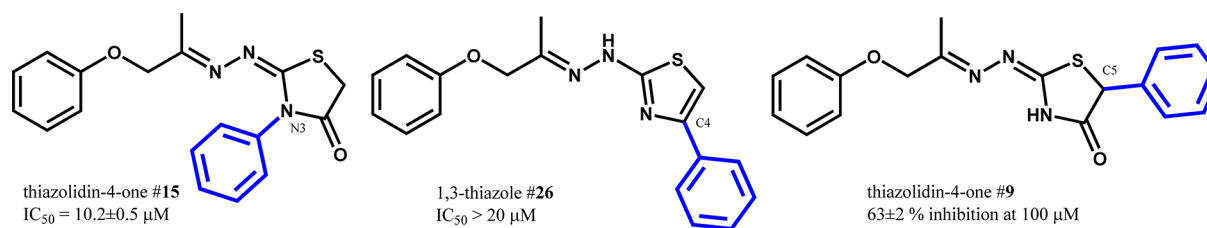


Figure 3. Structure–activity relationships of 2-iminothiazolidin-4-ones versus 2-imino-1,3-thiazoles. Biochemical data for cruzain.

Of all the tested compounds, 2-imino-1,3-thiazoles **29** and **36** possessed the highest overall trypanocidal potency. Compounds **29** and **36** had trypanocidal activity comparable to that of Bdz, with IC_{50} values of 3.9 and 3.8 μM for bloodstream Y strain trypomastigotes, respectively. 2-Imino-1,3-thiazole **29** was identified when the phenyl ring at C4 was replaced with a pyridine ring. Replacing phenyl (**26**) with a pyridine ring (compounds **27–29**) changes the magnitude of trypanocidal properties for Y strain trypomastigotes. A 2-pyridine ring (**27**) was less potent than a phenyl (**26**), but a 3-pyridine (**27**) and a 4-pyridine (**29**) increased the trypanocidal property without affecting mouse splenocytes. While appending a pyridine ring at C4 is beneficial, this is not the case when a 2-furfuryl (**42**) or a 2-thiophene (**43**) ring is attached.

We also analyzed the effect of para substitution on the phenyl ring. A 4-tolyl (**30**) is two times less cidal for trypomastigotes than phenyl (**26**), while a 4-methoxyphenyl (**31**) has the same potency as phenyl (**26**). When halogens were attached to the phenyl ring, a pronounced substituent effect was observed.³² 4-Fluorophenyl (**32**) is twice as toxic for trypomastigotes as phenyl thiazole (**26**) but still less potent than Bdz or Nfx. However, the same trypanocidal property was not observed when other halogen atoms were attached, such as 4-chloro (**33**), 4-bromo (**34**), or dichloro (**37–39**), all of them having poor trypanocidal properties. Dichloro (compounds **37** and **38**) and trichloro (**39**) thiazoles were also toxic to mouse splenocytes. However, inserting a nitro group at the para position (**35**) and ortho position (**36**) produced the most potent anti-*T. cruzi* thiazoles. For example, 4-nitrophenyl thiazole **35** inhibited the proliferation of epimastigotes (IC_{50} of 1.9 μM) and is toxic for trypomastigotes (IC_{50} of 5.7 μM) without affecting the cell viability of mouse splenocytes, i.e., nontoxic at 100 $\mu\text{g}/\text{mL}$ (271 μM).

Finally, we prepared and tested 2-imino-1,3-thiazoles containing a methyl (**44**) or phenyl (**45**) located at N3. In comparison to nonsubstituted 2-imino-1,3-thiazole **26**, which has $IC_{50} = 19.6 \mu\text{M}$ for trypomastigotes, thiazoles **44** and **45** exhibited an IC_{50} of 174.7 and 61.1 μM , respectively. This suggests that a NH is important for maintaining trypanocidal properties.

To sum up the SAR for 2-imino-1,3-thiazoles **26–45**, optimal trypanocidal thiazoles resulted when electron-withdrawing groups such as 4-fluoro, 3-nitro, and 4-nitro were attached to the phenyl ring at C4. Chloro, bromo, and dichloro proved to be detrimental. Electron-releasing groups such as methyl, methoxy, and *tert*-butyl are of little or no benefit when compared to nonsubstituted thiazole **26**. Exchanging phenyl (**26**) with a naphthyl group (**41**) is not good, **41** being half as potent as **26**.

Once we determined that *N*-phenyl 2-iminothiazolidin-4-ones **15–19**, **22–24** as well as 2-iminothiazolidin-4-thiones **20**, **21** inhibited the catalytic activity of cruzain to some degree, we wondered whether this inhibitory property was only for cruzain and not for other cysteine proteases. To this end, we assayed these compounds for inhibition of cathepsins L and S. At 100 μM , none the *N*-phenyl 2-iminothiazolidin-4-ones **15–19** and **22–24** inhibited cathepsins, while the 2-iminothiazolidin-4-thiones

20 and **21** inhibited cathepsins. As we can infer from Table 3, some of the *N*-phenyl 2-iminothiazolidin-4-ones, such as **17** and **18**, were at least 10 times more selective for cruzain than for cathepsins.

A referee suggested that the weak to moderate potency of 2-iminothiazolidin-4-ones in inhibiting cruzain may be caused by a nonspecific reactivity toward enzymatic nucleophiles or compound aggregation involving nonspecific attachment to the enzyme surface. The *N*-phenyl 2-iminothiazolidin-4-ones **15–19**, **22–24** do not possess general inhibitory properties for cysteine proteases; they only display inhibitory properties for cruzain. Therefore, a nonspecific reactivity toward enzymatic nucleophiles is not the case for these compounds. The same cannot be said for 2-iminothiazolidin-4-thiones **20** and **21**, which inhibit both cruzain and cathepsin without selectivity. But to ascertain that *N*-phenyl 2-iminothiazolidin-4-ones **15–19** and **22–24** do inhibit cruzain without compound aggregation, we needed to repeat some reactions by adding 0.01% of detergent.³¹ As shown in Table 3, cruzain inhibition by compounds **17**, **18**, or **20** was not altered once the detergent (Triton X-100) was added, reinforcing the notion that cruzain inhibition by 2-iminothiazolidin-4-ones is specific.

We also wanted to gain information about the cruzain inhibition in the parasite cells. However, there is no cruzain gene knockout *T. cruzi* cell culture, and the existing cruzain-deficient cell line is also resistant to cruzain inhibitors. To overcome this limitation, we decided to treat the parasite with the *N*-phenyl 2-iminothiazolidin-4-one **18** and examine the ultrastructural alterations as well as the protease activity.

Bloodstream trypomastigotes as well infected macrophages were treated with 3.9 μM **18** and examined with transmission electron microscopy (TEM) and scanning electron microscopy (SEM). This compound caused severe ultrastructural alterations in the parasite (for complete details, see the Figures S2 and S3 in Supporting Information). In particular, we saw an atypical morphology in the Golgi complex, such as dilation of cisternae and atypical vacuoles, which are characteristic alterations caused by cruzain inhibitors.³³

Besides the evidence collected with electron microscopy, we also gained information by performing zymography assays with epimastigotes. Epimastigotes were treated with the 2-iminothiazolidin-4-ones **18** and incubated for 48 h. The SDS-page gel containing 0.1% gelatin was loaded per slot with 20 μg of parasite protein. As seen in Figure S4 (Supporting Information), the nontreated epimastigote extract displayed proteolytic activity for gelatin, while the cells treated with the cruzain inhibitor E-64 or a protease inhibitor cocktail did not. The treatment of epimastigotes with the 2-iminothiazolidin-4-ones **18** reduces the proteolytic activity in a concentration-dependent manner.

Putative Binding Model. The cruzain inhibition of compounds **5–24** indicates that a hydrophobic substituent at C5, such as ethyl (**17**) and isopropyl (**8**, **13**, **18**), renders excellent cruzain inhibitors, better than if a phenyl is attached at

C5 (9, 19). These findings are consistent with another report showing that the attachment of a hydrophilic substituent at C5 in 2-iminothiazolidin-4-ones, such as *N*-methylacetamide and esters, does not enhance the inhibitory properties of 2-iminothiazolidin-4-ones with regard to cruzain.³⁴ In the case of position N3, a phenyl group is well tolerated, but a methyl (10, 11) and cyclohexyl (24) are not so well tolerated. To clarify these relationships, these compounds were investigated using molecular docking with cruzain.

The binding mode for these ligands was determined as the highest (most positive) score among the possible solutions for each ligand, generated according to the Goldscore Fitness Function. Figure 4 shows the superimposition of the best docking

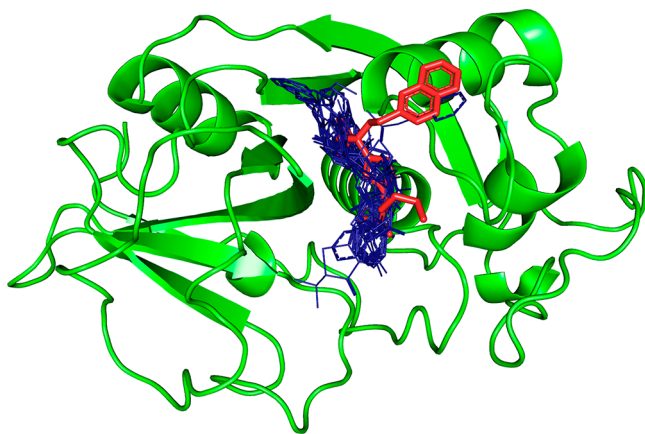


Figure 4. Superimposition of the docking solutions (blue lines) for compounds that have IC_{50} for cruzain: 8R, 8S, 12R, 12S, 13R, 13S, 15, 16R, 16S, 17R, 17S, 18R, 18S, 20R, 20S, 21R, 21S, 22R, 22S, 23R, 23S, and the crystallographic structure of the “KB2” (54) cocrystallized ligand (red-stick). Figure generated with Pymol.⁴⁹

solutions for compounds that have IC_{50} values experimentally determined for cruzain, which are: 8R, 8S, 12R, 12S, 13R, 13S, 15, 16R, 16S, 17R, 17S, 18R, 18S, 20R, 20S, 21R, 21S, 22R, 22S, 23R, 23S, and the crystallographic structure of the “KB2” (triazole 54) cocrystallized ligand. To compare in silico versus in vitro cruzain data, IC_{50} values were first converted into pIC_{50} values (equals $-\log IC_{50}$ for cruzain inhibition, at molar concentration).

Figure 5 shows the association observed between the in silico docking scores and the pIC_{50} data, which indicates that the most potent compounds, or the compounds with the highest values

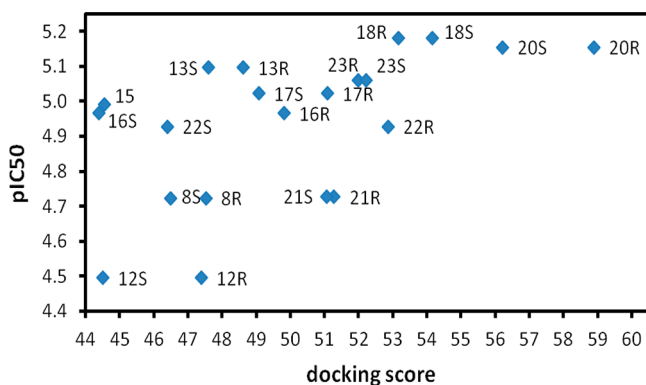


Figure 5. Trend observed between the in vitro (pIC_{50} for cruzain inhibition) and in silico (docking score) results. The S and the R symbols stand for the respective enantiomer.

for pIC_{50} , are usually those with the higher docking scores, demonstrating that the molecules with more stable or positive docking scores (i.e., greater in silico affinity for cruzain) are also the most potent cruzain inhibitors (i.e., greater in vitro pIC_{50} values).

To identify the molecular reasons for the two extremes of potency (highest and lowest in vitro results, 18S and 12R, respectively), we performed a detailed analysis of the intermolecular interactions. The enantiomer with higher in silico affinity was selected in each case. The differences between these two molecules are as follows: (i) the presence of a phenyl ring linked to the N3 nitrogen atom of the thiazolidinic ring in molecule 18S, instead of a methyl group in molecule 12R; (ii) an isopropyl group at position C5 of the thiazolidinic ring for molecule 18S, rather than an ethyl group for 12R. It seems that the additional hydrophobicity of the phenyl and isopropyl groups in 2-iminothiazolidin-4-one 18S provides a greater contact surface for interactions with cruzain hydrophobic residues, as shown in Figures 6 and 7.

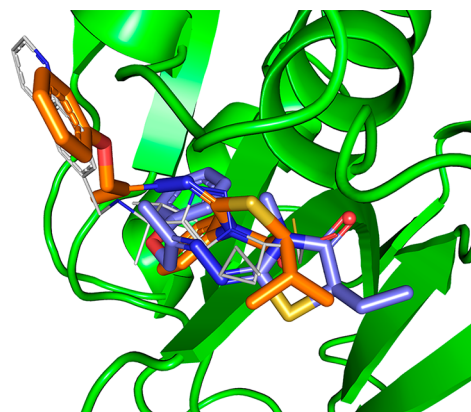


Figure 6. Superimposition of the docking solutions for compounds 12R (blue stick) and 18S (orange stick) and the crystallographic structure of the “KB2” (54) cocrystallized ligand (gray line).

The difference between the binding modes of these molecules is shown in detail in Figure 7 and Table 5. The hydrophobic residues are highlighted in green, those that participate in the hydrogen bond are highlighted in cyan, and π - π stacking interactions are highlighted in orange. The benzene ring linked to the N3 nitrogen atom is capable of forming a π - π interaction with the HIS162 amino acid residue, which may be a key interaction for positioning the phenoxy group close to SER61, SER64, GLY65, GLY66, and LEU67 residues, providing greater stability for the complex by way of hydrophobic contact and one hydrogen bond, highlighted in Figure 7B. These differences ensured that the docking solution for molecule 18S was the only one in the series of compounds that came closer to the crystal position of the “KB2” ligand, as shown in Figures 4 and 6.

In Vitro and in Vivo Infection. Given the selectivity of these compounds against extracellular forms of *T. cruzi*, we next examined the activity for the intracellular parasite. To this end, we assayed an in vitro model of parasite development using mouse macrophages infected with Y strain trypomastigotes. Four days postinfection, untreated control had 35–40% of macrophages infected and a high mean number of intracellular amastigotes. In this assay, 10 μ M Bdz reduces roughly half of infected cells as well the number of intracellular amastigotes, indicating a severe impairment of parasite development. Once we had this assay validated, we first tested the three most potent

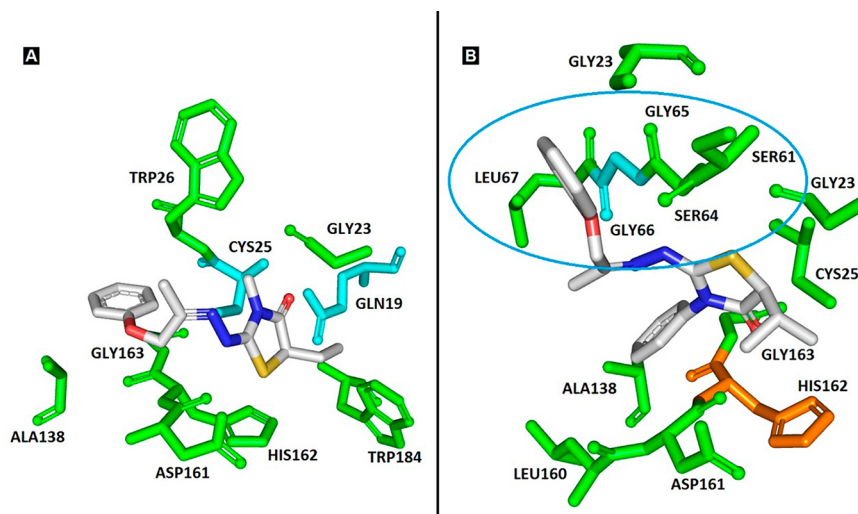


Figure 7. Detailed view of the docking solutions for (A) compound **12R** and (B) compound **18S**. Hydrophobic interactions (green), hydrogen bonds (cyan), and the π - π interactions (orange). The highlighted residues (blue circle) interacting with molecule **18S** are involved with the additional intermolecular interactions responsible for the greater affinity of this inhibitor, as shown in Table 5.

Table 5. Molecular Interaction of Cruzain with Molecules 12R and 18S^a

cruzain residues	molecules	
	12R	18S
GLN19	3.0	
GLY23	HC	HC
CYS25	2.5	HC
TRP26	HC	
SER61		HC
SER64		HC
GLY65		HC
GLY66		2.9
LEU67		HC
ALA138	HC	HC
LEU160		HC
ASP161	HC	HC
HIS162	HC	PI
GLY163	HC	HC
TRP184	HC	

^aHC means hydrophobic contacts, PI means π - π stacking, and the numbers are the hydrogen bond distances in angstroms.

cruzain inhibitors, 2-iminothiazolidin-4-ones **16**, **17**, and **18** as well as the 2-imino-1,3-thiazoles **29** and **35**.

At a concentration of 10 μ M, we observed that 2-iminothiazolidin-4-one **18** was able to reduce the number of infected cells with efficacy more pronounced than that seen with Bdz-treated cells. 2-Iminothiazolidin-4-ones **16** and **17** were less potent than Bdz. 2-Imino-1,3-thiazole **29**, which was a trypanocidal compound for bloodstream parasites, had no significant activity in reducing the infection in macrophages. Yet 4-nitro derivative **35** inhibited the in vitro infection similarly to Bdz (Table S1, Supporting Information).

We next examined the 2-iminothiazolidin-4-ones **5** and **18** at a concentration of 50 μ M. As seen in Figure 8A and B, compound **18** as well as Bdz substantially reduces the intracellular parasites in most of the microscopy fields ($P < 0.001$). We determined the IC₅₀ values of these compounds to reduce the percentage of infected macrophages (Table 6), and we found that 2-iminothiazolidin-4-one **18** has an IC₅₀ of 10.1 \pm 0.09 μ M, almost identical to that of Bdz

(IC₅₀ of 13.9 \pm 0.39 μ M). 2-Iminothiazolidin-4-one **5**, which had an IC₅₀ of 19.0 μ M for bloodstream parasites but did not inhibit cruzain, showed an IC₅₀ of 19.5 \pm 1.1 μ M to reduce the percentage of infected macrophages.

Table 1 shows that in concentrations up to 100 μ g/mL (262 μ M), the 2-iminothiazolidin-4-one **18** does not affect cell viability of mouse splenocytes. We next wanted to determine the IC₅₀ value. Strikingly, compound **18** does not affect either cell viability or proliferation (under mitogen challenge) of splenocytes (IC₅₀ values >262 μ M), in contrast to an IC₅₀ of 10.1 \pm 0.09 μ M for intracellular *T. cruzi* (Table 6). The selectivity index (SI) value can be estimated to be over 25. For comparison, compound **5**, our simplest 2-iminothiazolidin-4-one variant, has an SI of 10.

On the one hand, we have potency enhancement from 2-iminothiazolidin-4-one **5** to **18** (Table 6). On the other hand, we have observed that even at a concentration of 50 μ M, 2-iminothiazolidin-4-one **18** does not eradicate the infection in a culture of macrophages. The same is observed under treatment with Bdz. As seen in Figure 8C, we only approached eradication of the in vitro intracellular parasite under the simultaneous treatment of Bdz and **18**.

Chemically inhibiting parasite invasion is a desirable functional property for any Chagas disease drug candidate. For that reason, we assayed an invasion experiment with Y strain trypomastigotes in mouse macrophages.³⁵ After 60 min of parasite exposure, about 35% of macrophages are infected (untreated control). Bdz did not impair parasite viability in the invasion assay, even at 50 μ M; so we decided to use amphotericin B (AmpB) as a reference drug. At 50 μ M, AmpB was quite efficient in inhibiting parasite invasion into macrophages. Our best cruzain and *T. cruzi* inhibitor, *N*-phenyl 2-iminothiazolidin-4-one **18**, also decreased parasite invasion ($P < 0.01$) albeit less than AmpB did. 2-Iminothiazolidin-4-one **5** only attenuated the invasion ($P < 0.05$), and thiazole **29** did not have any significant effect in this assay (Figure 8D).

Finally, we evaluated the in vivo efficacy of *N*-phenyl 2-iminothiazolidin-4-one **18** to reduce blood parasitemia (acute phase). Starting on day 5 postinfection (dpi), compound **18** was orally administered once a day at 250 μ mol/kg for 5 consecutive days in BALB/c mice infected with 10⁴ Y strain trypomastigotes. Controls included untreated and Bdz-treated infected mice.

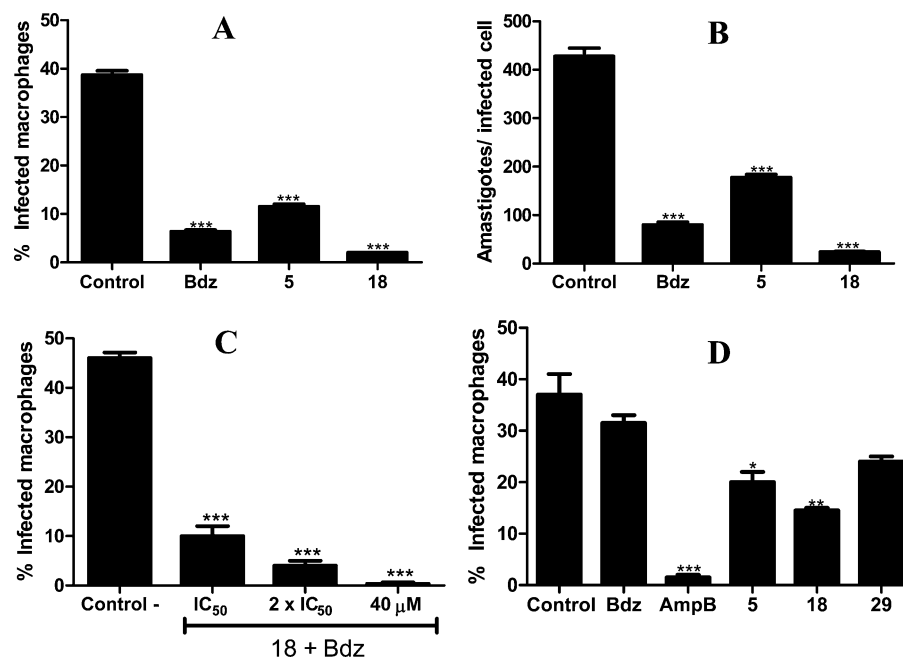


Figure 8. 2-Iminothiazolidin-4-one **18** severely impairs intracellular parasite development. The infection ratio (A) and the mean number of intracellular amastigotes per host cell (B) are higher in untreated controls than in cultures treated with test inhibitors **5**, **18**, or Bdz. Macrophages were infected with Y strain trypomastigotes for 2 h, and test inhibitors were then added at 50 μM . Cell cultures were incubated for 4 days. Significance: ***, $P < 0.001$; *, $P < 0.01$. (C) Combined treatment of 2-iminothiazolidin-4-one **18** (40 μM) and Bdz (40 μM) approaches an eradication of in vitro infection. Macrophages were infected with Y strain trypomastigotes for 2 h, and the combination of drugs was simultaneously added. Cell cultures were incubated for 4 days. Significance: ***, $P < 0.001$. (D) 2-Iminothiazolidin-4-one **18** attenuates parasite invasion in host cells, while Bdz does not. Y strain trypomastigotes and each test inhibitor (at 50 μM) were simultaneously added to the cell culture of macrophages and incubated for 2 h. ***, $P < 0.001$; **, $P < 0.01$; *, $P < 0.05$. All test inhibitors were tested in triplicate concentrations, and two independent experiments were carried out. Standard deviations are shown as error bars. Bdz is benznidazole; AmpB is amphotericin B.

Table 6. Comparison of the Pharmacological Properties between the 2-Iminothiazolidin-4-ones **5 and **18****

compd	IC_{50} ($\pm\text{SD}$), μM				
	intracellular parasite ^a	toxicity for splenocytes ^b	antiproliferative for splenocytes ^c	index (SI) ^d	% parasitemia reduction in mice ^e
5	19.5 \pm 1.1	>200	98 \pm 10	10	—
18	10.1 \pm 0.09	>262	>262	25	89.6
controls	13.9 \pm 0.39 (benznidazole)	1.7 \pm 0.002 (saponin)	0.01 $\mu\text{g}/\text{mL}$ (cyclosporine A)	—	>99 (benznidazole)

^aDetermined 4 days after incubation of infected macrophages. IC_{50} values calculated in regard to the percent of treated infected cells in comparison to untreated infected cells. ^bDetermined 24 h after incubation of mouse splenocytes. Cell viability measured using the incorporation of tritiated thymidine. ^cSplenocyte proliferation was induced by concanavalin A. The effect on the proliferation was determined 72 h after incubation of mouse splenocytes using the AlamarBlue. SD is the standard deviation. ^dCellular selective index was estimated using the ratio (IC_{50} for splenocytes)/(IC_{50} for amastigotes). ^eCalculated as [(average vehicle group – average treated group)/average vehicle group] \times 100%. Values of blood parasitemia were taken from day 5 of treatment.

The course of infection was monitored by counting blood parasites in a hemocytometer, and animal survival was followed for one month.³⁶ As seen in Figure 9 and Table 6, compound **18** was efficient in reducing 89.6% of blood parasitemia ($P < 0.001$ of significance) when compared to untreated control. Bdz was even more effective than **18**, nearly eradicating blood parasites (>99% of parasitemia reduction). No signs of toxicity or body weight loss were observed in mice of the treatment groups.

DISCUSSION

Thiosemicarbazones are known for their powerful in vitro trypanocidal and cruzain inhibition effects.^{13–17} However, currently, very few thiosemicarbazones that are effective in reducing in vivo *T. cruzi* infection have been described.³⁷ One method for increasing the efficacy of anti-*T. cruzi* thiosemicarbazones is through complexation with transition metals.^{38–40} Another possibility is the chemical modification of thiosemicarbazones by

synthetic redesign. We found that 2-iminothiazolidin-4-ones are structural analogues of thiosemicarbazones and endowed with in vitro trypanocidal properties. In previous studies, we discovered that 2-iminothiazolidin-4-ones were less potent trypanocidal agents than thiosemicarbazones, but at least 2-iminothiazolidin-4-ones were more selective for parasite than for mammalian cells.^{25–27} Here, our principal aim was to improve the cidal potency by molecular modification. We knew from past studies that the thiazolidinidic ring is more important for trypanocidal activity than the hydrazone and aryl groups. We chose the aryloxypropylimine group as a common core for designing compounds **5–45** because of the remarkable functional property of the drug candidate aryloxymethyl ketone triazole **54**.²³ We next wanted to identify the main structural determinants for trypanocidal and cruzain inhibition in this class of 2-iminothiazolidin-4-ones. Here, we have identified most of them after screening the 2-iminothiazolidin-4-ones **5–24** and comparing them with 2-imino-1,3-thiazoles **26–45**.

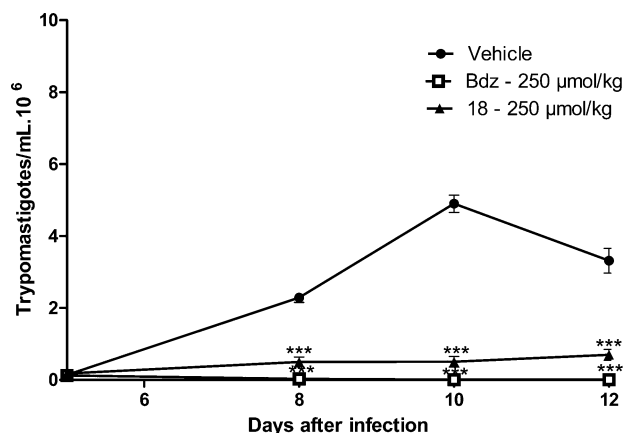


Figure 9. 2-Iminothiazolidin-4-one **18** substantially reduces the parasitemia in mice. Female BALB/c mice were infected with 10^4 Y strain trypomastigotes. Five days postinfection (dpi) mice were orally treated once a day with compound **18** or benznidazole (Bdz) at a dose of $250 \mu\text{mol/kg}$ during five consecutive days. Parasitemia was monitored by counting the number of trypomastigotes in fresh blood samples. Values represent the mean \pm SEM of six mice per group. Two independent experiments; data are representative from one experiment. Significance (***, $P < 0.0001$) compared to untreated infected group (vehicle).

We first observed that, with few exceptions, most of the nonsubstituted 2-iminothiazolidin-4-ones **5–9** or those containing a methyl at N3 **10–14** are inactive or poor cruzain inhibitors, and there was no reliable relationship between trypanocidal effects and chemical structure. In contrast, 2-iminothiazolidin-4-ones containing a phenyl group at N3 (**15–19**, **22–24**) inhibit cruzain and share trypanocidal properties. They are effective against the parasite but with the notable advantage that they do not affect either the viability or the proliferation of host cells.

With regard to the mechanism of action, we cannot confirm whether the anti-*T. cruzi* property is entirely due to the inhibition of cruzain alone. We argue that the trypanocidal properties of compounds **15–24** are, to some degree, a result of cruzain inhibition. This statement is based on the ability of 2-iminothiazolidin-4-ones to inhibit the catalytic activity of recombinant cruzain (competition experiments), to alter the morphology of the Golgi complex (electron microscopy), and to impair the proteolytic activity in the whole parasite (zymography assays with epimastigotes).

The model of docking for 2-iminothiazolidin-4-one **18** with cruzain shows that the phenyl ring linked to the N3 nitrogen is capable of forming a π - π interaction with the HIS162 amino acid. This interaction would seem to be the reason for the phenoxy group being located at a position which allows important hydrophobic contacts and hydrogen bond interactions, giving greater stability to the complex. The same is not predicted for 2-iminothiazolidin-4-one containing a methyl at N3, such as compound **12**. This model is consistent with recombinant cruzain inhibition and also provides an explanation for why the attachment of the phenyl on the heterocyclic ring is important for cruzain inhibition, in addition to explaining the importance of an alkyl group, such as ethyl and isopropyl, at position C5.

Despite the structural analogy, the functional properties of 2-iminothiazolidin-4-ones **5–24** and 2-imino-1,3-thiazoles **26–45** are distinguishable. 2-Iminothiazolidin-4-ones inhibited the catalytic activity of cruzain while none of the tested thiazoles did. Therefore, they do not behave as antiparasitic bioisosteres.

Our findings corroborate a very recent work describing that 2-imino-1,3-thiazoles are trypanocidal agents by altering the ergosterol biosynthesis instead of inhibiting the catalytic activity of cruzain.⁴¹ In agreement with this, we also found 2-imino-1,3-thiazoles are trypanocidal agents, and a few of them were equipotent to Bdz, such as thiazoles **29**, **35**, and **36**. There was a clear trend toward trypanocidal potency as polar substituents on the phenyl at C4 are attached to 2-imino-1,3-thiazoles. This led to some of the most potent thiazole variants examined, such as compounds **29** (4-pyridine), **32** (4-fluor), **35** (4-nitro), and **36** (3-nitro). This contrasts with the incorporation of an alkyl (**30**, **31**, **40**) or naphthyl (**41**) group, which, in the same position, decreased the cidal effects of the thiazole.

The selectivity of 2-iminothiazolidin-4-ones seems to be more consistent than that of 2-imino-1,3-thiazoles, because some thiazole variants were toxic to mouse splenocytes. Moreover, the mechanism through which thiazoles arrest parasite growth remains unknown. In view of these findings, we decided to search for more information on the trypanocidal effects of 2-iminothiazolidin-4-ones. We selected 2-iminothiazolidin-4-one **18**, the most potent cruzain inhibitor among the examined compounds. With regard to the functional activity of **18**, it inhibits the catalytic activity of cruzain but not that of cathepsins L and S, clearly arrests parasite growth (epimastigotes) and motility (trypomastigotes), impairs intracellular trypomastigote development into amastigotes, and attenuates trypomastigote invasion of macrophages. Using electron microscopy, we observed that 2-iminothiazolidin-4-one **18** alters the parasite morphology, in particular, altering the structure of the Golgi complex in a way very similar to that for other cruzain inhibitors. Moreover, 2-iminothiazolidin-4-one **18** reduces the protease activity in epimastigotes; both experiments suggest that cruzain is involved with the trypanocidal activity of 2-iminothiazolidin-4-one **18**. Finally, the antiparasitic effect of compound **18** was reinforced by its efficacy in reducing blood parasitemia in *T. cruzi*-infected mice.

One potential downside to **18** is that it does not eradicate parasitemia in mice (acute infection), a desirable property already demonstrated for other Chagas disease drug candidates.^{23,42–44} However, the design of anti-*T. cruzi* 2-iminothiazolidin-4-one **18** is a remarkable achievement for our program, especially because it worked orally. Synthetic redesign of the aryloxypropylimine group is one possible way to optimize the efficacy of compound **18**.

CONCLUSIONS

A detailed SAR study of anti-*T. cruzi* 2-iminothiazolidin-4-ones was conducted. It included molecular modifications on the thiazolidinic ring, as well isosteric exchanges of the carbonyl carbon and of the heterocycle itself. We observed a remarkable improvement in trypanocidal properties and cruzain inhibition only when positions N3 and C5 in the thiazolidinic ring were simultaneously substituted. This led to the identification of potent *N*-phenyl 2-iminothiazolidin-4-ones **15–19**, **22–24**. Replacement of the carbonyl with thiocarbonyl (**20**, **21**) did not produce a clear enhancement in potency, and exchanging the thiazolidinic for a thiazole ring **26–45** was deleterious for cruzain affinity, although some thiazoles did exhibit trypanocidal properties. Of compounds **15–24**, we found consistent trypanocidal effects for **18**, thereby corroborating the notion that this class of heterocycles can lead to useful cidal agents for Chagas disease treatment.

EXPERIMENTAL SECTION

Equipment and Reagents. All reagents were used as purchased from commercial sources (Sigma-Aldrich, Acros Organics, Vetec, or Fluka). Moisture-sensitive reactions were carried out under a nitrogen atmosphere. Progress of the reactions was followed by thin-layer chromatography (silica gel 60 F₂₅₄ in aluminum foil). Purity of the target compounds was confirmed by combustion analysis (for C, H, N, S) performed by a Carlo-Erba instrument (model EA 1110). Chemical identity was confirmed with NMR and IR spectroscopy and accurate mass. IR was determined in KBr pellets. For NMR, we used a Varian UnityPlus 400 MHz (400 MHz for ¹H and 100 MHz for ¹³C) and Bruker AMX-300 MHz (300 MHz for ¹H and 75.5 MHz for ¹³C) instruments. DMSO-*d*₆, acetone-*d*₆, CDCl₃, and D₂O were purchased from CIL or Sigma-Aldrich. Chemical shifts are reported in ppm, and multiplicities are given as s (singlet), d (doublet), t (triplet), q (quartet), m (multiplet), and dd (doublet), and coupling constants (*J*) in hertz. NH signals were localized in each spectrum after the addition of a few drops of D₂O. Structural assignments were corroborated by DEPT, HMBC and HSBC experiments. Mass spectrometry experiments were performed on a Q-TOF spectrometer (nanoUPLC-Xevo G2 Tof, Waters) or LC-IT-TOF (Shimadzu). When otherwise specified, ESI was carried out in the positive ion mode. Typical conditions were capillary voltage of 3 kV, cone voltage of 30 V, and a peak scan between 50 and 1000 *m/z*. To determine the molecular structure of thiosemicarbazones **4a** and **4c** as well as 2-iminothiazolidin-4-one **12**, a crystal of the corresponding compound was mounted on a Enraf-Nonius Kappa diffractometer equipped with a CCD detector (95 mm camera on κ -goniostat), and reflections were measured using monochromatic Mo K α radiation (0.71073 Å) at room temperature.

General Procedure for the Synthesis of 2-Iminothiazolidin-4-ones 5–19 and 22–24. Example for compound 5: Thiosemicarbazone **4a** (1.12 g, 5 mmol), anhydrous sodium acetate (1.2 g, 15 mmol), and 100 mL of ethanol were added to a 250 mL round-bottom flask under magnetic stirring and slightly warmed for 10–15 min. Then ethyl 2-bromoacetate (1.6 g, 10 mmol) was added, and the colorless reaction was refluxed for 18 h. After cooling back to rt, the precipitate was filtered off and the solvent was evaporated to half of its volume and then cooled to 0 °C. A white solid was obtained, filtered in a Büchner funnel with a sintered disc filter, washed with cold water, and then dried over SiO₂. Products were purified by column chromatography or recrystallization using the solvent system detailed below for each compound. Purity of compounds were >95% as determined by combustion analysis.

2-((1-Phenoxypropan-2-ylidene)hydrazono)thiazolidin-4-one (5). After elution with hexane/toluene (1:1), colorless crystals were obtained, yield = 0.7 g, 53%. Mp (°C): 130–131. IR (KBr): 3196 (N–H), 3006 (C–H), 1734 (C=O), 1649 and 1595 (C=N) cm⁻¹. ¹H NMR (300 MHz, DMSO-*d*₆): δ 1.98 (s, 3H, CH₃), 3.83 (s, 2H, S–CH₂), 4.66 (s, 2H, CH₂), 6.92–6.99 (m, 3H, Ar), 7.28 (t, 2H, Ar), 11.90 (s, 1H, NH). ¹³C NMR (75.5 MHz, DMSO-*d*₆): δ 14.8 (CH₃), 32.8 (CH₂, heterocycle), 70.9 (CH₂), 114.5 (CH, Ar), 120.9 (CH, Ar), 129.5 (CH, Ar), 158.1 (C=N), 161.9 (C–O, Ar), 164.1 (S–C=N), 173.9 (C=O). HRMS (ESI): 286.0599 [M + Na]⁺. Anal. Calcd for C₁₂H₁₃N₃O₂S: C, 54.74; H, 4.98; N, 15.96; S, 12.18. Found: C, 54.42; H, 5.02; S, 11.91; N, 15.78.

2-((1-Phenoxypropan-2-ylidene)hydrazono)-5-methylthiazolidin-4-one (6). After elution with hexane/ethyl acetate (3:1), yellowish crystals were obtained, yield = 0.11 g, 33%. Mp (°C): 117–120. IR (KBr): 3195 (N–H), 1710 (C=O), 1640 and 1602 (C=N) cm⁻¹. ¹H NMR (300 MHz, DMSO-*d*₆): δ 1.46 (d, 3H, J 7.8 Hz, CH₃), 2.02 (s, 3H, CH₃), 4.11 (t, 1H, J 7.8 Hz, CH), 4.66 (s, 2H, CH₂), 6.93–6.99 (m, 3H, Ar), 7.28 (t, 2H, Ar), 11.79 (s, 1H, NH). ¹³C NMR (75.5 MHz, DMSO-*d*₆): δ 14.5 (CH₃), 18.6 (CH₃), 41.7 (CH), 70.9 (CH₂), 114.6 (CH, Ar), 120.8 (CH, Ar), 129.3 (CH, Ar), 158.0 (C=N), 161.8 (C–O, Ar), 161.9 (S–C=N), 176.5 (C=O). HRMS (ESI): 278.0995 [M + H]⁺. Anal. Calcd for C₁₃H₁₅N₃SO₂: C, 56.30; H, 5.45; N, 15.15; S, 11.56. Found: C, 56.16; H, 5.38; S, 11.21; N, 15.09.

2-((1-Phenoxypropan-2-ylidene)hydrazono)-5-ethylthiazolidin-4-one (7). After elution with hexane/toluene (2:1), yellowish crystals were obtained, yield = 0.15 g, 51%. Mp (°C): 133. IR (KBr): 1715 (C=O), 1614 and 1596 (C=N) cm⁻¹. ¹H NMR (400 MHz, DMSO-*d*₆): δ 0.94

(t, J 7.2 Hz, 3H, CH₃), 1.73–1.81 (m, 1H, J 7.2 and 4.4 Hz, CH₂), 1.92–1.98 (m, 1H, J 7.2 and 4.4 Hz, CH₂), 2.02 (s, 3H, CH₃), 4.12–4.15 (q, 1H, J 7.6 and 4.4 Hz, CH asymmetric), 4.67 (s, 2H, CH₂), 6.92–7.00 (m, 3H, Ar), 7.28 (t, 2H, Ar), 11.94 (broad s, 1H, NH). ¹³C NMR (100 MHz, DMSO-*d*₆): 10.1 (CH₃), 14.5 (CH₃), 25.4 (CH₂), 48.8 (CH), 70.9 (CH₂), 114.6 (CH, Ar), 120.8 (CH, Ar), 129.3 (CH, Ar), 158.1 (C=N), 161.9 (C–O, Ar), 162.1 (S–C=N), 175.6 (C=O). Anal. Calcd for C₁₄H₁₇N₃SO₂: C, 57.71; H, 5.88; N, 14.42; S, 11.00; found: C, 57.64; H, 5.69; N, 14.25; S, 10.89.

2-((1-Phenoxypropan-2-ylidene)hydrazono)-5-isopropylthiazolidin-4-one (8). Crystallization from cyclohexane afforded colorless crystals, yield = 0.14 g, 38%. Mp (°C): 139. IR (KBr): 2967 (C–H), 1725 (C=O), 1640 and 1580 (C=N) cm⁻¹. ¹H NMR (400 MHz, DMSO-*d*₆): δ 0.86 (d, 3H, J 4.0 Hz, CH₃), 0.96 (d, 3H, J 4.0 Hz, CH₃), 1.97 and 2.01 (two s, 3H, CH₃), 2.35 (broad s, 1H, CH), 4.25 (s, 1H, CH), 4.61 and 4.67 (two s, 2H, CH₂), 6.98 (t, 3H, Ar), 7.28 (d, 2H, Ar), 11.86 (s, 1H, NH). ¹³C NMR (100 MHz, DMSO-*d*₆): 14.7 (CH₃), 16.2 (CH₃), 20.2 (CH₃), 29.8 (CH), 54.4 (CH), 70.9 (CH₂), 114.7 (CH, Ar), 120.9 (CH, Ar), 129.4 (Ar), 158.1 (C=N), 162.1 (C), 175.2 (C=O). HRMS (ESI): 306.1265 [M + H]⁺. Anal. Calcd for C₁₅H₁₉N₃SO₂: C, 58.99; H, 6.27; N, 13.76; S, 10.50; found: C, 59.53; H, 6.21; S, 8.69; N, 13.38.

2-((1-Phenoxypropan-2-ylidene)hydrazono)-5-phenylthiazolidin-4-one (9). Crystallization from toluene afforded colorless crystals, yield = 0.14 g, 41%. Mp (°C): 150. IR (KBr): 3391 (N–H), 1709 (C=O), 1640 and 1599 (C=N) cm⁻¹. ¹H NMR (400 MHz, acetone-*d*₆): δ 1.92 and 2.06 (s, 3H, CH₃), 3.58 (br s, NH+HDO), 4.67 and 5.01 (s, 2H, CH₂), 5.34 (s, 1H, CH), 6.90–7.01 (m, 3H, Ar), 7.27 (br s, 7H, Ar). ¹³C NMR and DEPT (100 MHz, acetone-*d*₆): 14.8 and 26.3 (CH₃), 51.4 (CH), 65.1 and 71.0 (CH₂), 114.2 (CH, Ar), 114.2 (CH, Ar), 120.9 (CH, Ar), 128.3 (CH, Ar), 128.7 (CH, Ar), 129.4 (CH, Ar), 130.4 (CH, Ar), 137.4 (C–N, Ar), 157.0 and 157.1 (C=N), 161.2 and 162.8 (C–O, Ar), 164.4 (S–C=N), 176.1 (C=O). HRMS (ESI): 340.1129 [M + H]⁺. Anal. Calcd for C₁₈H₁₇SO₂N₃: C, 63.70; H, 5.05; N, 12.38; S, 9.45; found: C, 64.01; N, 12.60; H, 5.60; S, 8.73.

2-((1-Phenoxypropan-2-ylidene)hydrazono)-3-methylthiazolidin-4-one (10). Crystallization from cyclohexane afforded colorless crystals, yield = 0.15 g, 54%. Mp (°C): 112. IR (KBr): 1721 (C=O), 1636 and 1580 (C=N) cm⁻¹. ¹H NMR (400 MHz, DMSO-*d*₆): δ 2.06 (s, 3H, CH₃), 3.13 (s, 3H, N–CH₃), 3.87 (s, 2H, CH₂), 4.70 and 5.02 (two s, 2H, CH₂–O), 6.94–7.00 (m, 3H, Ar), 7.27–7.30 (m, 2H, Ar). ¹³C NMR (100 MHz, DMSO-*d*₆): 14.4 and 19.4 (CH₃), 29.2 (N–CH₃), 31.9 (CH₂), 64.9 and 70.8 (CH₂), 114.2 (CH, Ar), 114.7 (CH, Ar), 120.9 (CH, Ar), 129.4 (CH, Ar), 158.0 (C=N), 163.1 (C), 172.0 (C=O). HRMS (ESI): 278.0995 [M + H]⁺. Anal. Calcd for C₁₃H₁₅N₃SO₂: C, 56.30; H, 5.45; N, 15.15; S, 11.56; found: C, 56.54; H, 5.40; S, 9.89; N, 14.91.

2-((1-Phenoxypropan-2-ylidene)hydrazono)-3,5-dimethylthiazolidin-4-one (11). Crystallization from toluene afforded colorless crystals, yield = 0.18 g, 60%. Mp (°C): 67. IR (KBr): 1720 (C=O), 1632 (C=N), 1581 (C=N) cm⁻¹. ¹H NMR (300 MHz, DMSO-*d*₆): δ 1.48 (d, 3H, J 7.2 Hz, CH₃), 2.06 (s, 3H, CH₃), 3.14 (s, 3H, N–CH₃), 4.16–4.23 (q, 1H, J 7.2 Hz, CH), 4.69 (s, 2H, CH₂), 6.92–7.00 (m, 3H, Ar), 7.26–7.31 (m, 2H, Ar). ¹³C NMR (75.5 MHz, DMSO-*d*₆): 14.6 (CH₃), 18.7 (CH₃), 29.4 (N–CH₃), 41.2 (CH), 70.8 (CH₂), 114.7 (CH, Ar), 120.9 (CH, Ar), 129.4 (CH, Ar), 158.1 (C=N), 161.9 (C–O, Ar), 163.3 (S–C=N), 175.1 (C=O). HRMS (ESI): 292.1134 [M + H]⁺. Anal. Calcd for C₁₄H₁₇N₃SO₂: C, 57.71; H, 5.88; N, 14.42; S, 11.00; found: C, 57.70; H, 5.91; N, 14.38; S, 11.10.

2-((1-Phenoxypropan-2-ylidene)hydrazono)-3-methyl-5-ethylthiazolidin-4-one (12). Crude was washed with ethyl ether, affording colorless crystals, yield = 0.26 g, 76%. Mp (°C): 129. IR (KBr): 1718 (C=O), 1636 and 1582 (C=N) cm⁻¹. ¹H NMR (300 MHz, DMSO-*d*₆): δ 0.92 (t, 3H, J 7.5 Hz, CH₃), 1.74–1.82 (m, 1H, CH₂), 1.95–1.98 (m, 1H, CH₂), 2.06 (s, 3H, N–CH₃), 3.18 (s, 3H, N–CH₃), 4.21–4.25 (q, 1H, J 4.2 and 7.8 Hz, CH), 4.70 (s, 2H, CH₂), 6.93–7.01 (m, 3H, Ar), 7.26–7.32 (m, 2H, Ar). ¹³C NMR (75.5 MHz, DMSO-*d*₆): 10.3 (CH₃), 14.6 (CH₃), 25.5 (CH₂), 29.3 (N–CH₃), 48.2 (CH), 70.8 (CH₂), 114.7 (CH, Ar), 120.9 (CH, Ar), 129.5 (CH, Ar), 158.0 (C=N), 161.9 (C–O, Ar), 163.4 (S–C=N), 174.2 (C=O). HRMS (ESI): 306.1283

[M + H]⁺. Anal. Calcd for C₁₅H₁₉N₃O₂S: C, 58.99; N, 13.76; H, 6.27; S, 10.50; found: C, 59.15; H, 6.09; N, 13.32; S, 9.43.

2-((1-Phenoxypropan-2-ylidene)hydrazono)-3-methyl-5-isopropylthiazolidin-4-one (**13**). Crystallization from cyclohexane afforded colorless crystals, yield = 0.25 g, 70%. Mp (°C): 138. IR (KBr): 1717 (C=O), 1634 and 1581 (C=N) cm⁻¹. ¹H NMR (300 MHz, DMSO-*d*₆): δ 0.80 (d, 3H, *J* 6.6 Hz, CH₃), 0.97 (d, 3H, *J* 6.9 Hz, CH₃), 2.07 (s, 3H, CH₂), 2.39–2.42 (m, 1H, CH), 3.151 and 3.34 (s, 3H, N–CH₃), 4.31 (d, 1H, *J* 3.9 Hz, CH), 4.70 (s, 2H, CH₂), 6.92–7.00 (m, 3H, Ar), 7.26–7.31 (m, 3H, Ar). ¹³C NMR (75.5 MHz, DMSO-*d*₆): 14.5 (CH₃), 16.4 (CH₃), 20.2 (CH₃), 30.4 (CH), 31.3 (CH₃–N), 53.7 (CH), 70.8 (CH₂), 114.7 (CH, Ar), 120.9 (CH, Ar), 129.4 (CH, Ar), 158.1 (C=N), 161.9 (C–O, Ar), 163.5 (S–C=N), 173.7 (C=O). HRMS (ESI): 320.0915 [M + H]⁺. Anal. Calcd for C₁₆H₂₁N₃SO₂: C, 60.16; H, 6.63; N, 13.16; S, 10.04; found: C, 60.40; H, 6.14; N, 13.11; S, 9.66.

2-((1-Phenoxypropan-2-ylidene)hydrazono)-3-methyl-5-phenylthiazolidin-4-one (**14**). Crystallization from toluene afforded colorless crystals, yield = 0.25 g, 70%. Mp (°C): 157. IR (KBr): 1716 (C=O), 1628 and 1589 (C=N) cm⁻¹. ¹H NMR (300 MHz, DMSO-*d*₆): 1.98 and 2.12 (s, 3H, CH₃), 3.23 and 3.36 (s, 3H, N–CH₃), 4.71 (s, 2H, CH₂), 5.49 (s, 1H, CH), 6.94–7.00 (m, 3H, Ar), 7.25–7.30 (m, 3H, Ar), 7.37 (br s, 4H, Ar). ¹³C NMR (75.5 MHz, DMSO-*d*₆): 14.7 (CH₃), 26.3 and 29.8 (N–CH₃), 50.0 (CH), 70.7 (CH₂), 114.7 (CH, Ar), 120.9 (CH, Ar), 128.3 (CH, Ar), 128.5 (CH, Ar), 128.8 (CH, Ar), 129.4 (CH, Ar), 136.5 (C–N, Ar), 158.0 (C=N), 161.5 (C–O, Ar), 163.8 (S–C=N), 172.9 (C=O). HRMS (ESI): 354.0728 [M + H]⁺. Anal. Calcd for C₁₉H₁₉SO₂N₃: C, 64.57; H, 5.42; N, 11.89; S, 9.07; found: C, 64.41; N, 12.01; H, 5.39; S, 9.13.

2-((1-Phenoxypropan-2-ylidene)hydrazono)-3-phenylthiazolidin-4-one (**15**). Crystallization from toluene afforded colorless crystals, yield = 0.25 g, 70%. Mp (°C): 139. IR (KBr): 1716 (C=O), 1628 and 1589 (C=N) cm⁻¹. ¹H NMR (300 MHz, DMSO-*d*₆): 1.98 and 2.12 (s, 3H, CH₃), 3.23 and 3.36 (s, 3H, N–CH₃), 4.71 (s, 2H, CH₂), 5.49 (s, 1H, CH), 6.94–7.00 (m, 3H, Ar), 7.25–7.30 (m, 3H, Ar), 7.37 (broad s, 4H, Ar). ¹³C NMR (75.5 MHz, DMSO-*d*₆): 14.7 (CH₃), 26.3 and 29.8 (N–CH₃), 50.0 (CH), 70.7 (CH₂), 114.7 (CH, Ar), 120.9 (CH, Ar), 128.3 (CH, Ar), 128.5 (CH, Ar), 128.8 (CH, Ar), 129.4 (CH, Ar), 136.5 (C–N, Ar), 158.0 (C=N), 161.5 (C–O, Ar), 163.8 (S–C=N), 172.9 (C=O). HRMS (ESI): 354.0728 [M + H]⁺. Anal. Calcd for C₁₈H₁₇SO₂N₃: C, 63.70; H, 5.05; N, 12.38; S, 9.45; found: C, 63.65; N, 12.28; H, 5.13; S, 10.31.

2-((1-Phenoxypropan-2-ylidene)hydrazono)-3-phenyl-5-methylthiazolidin-4-one (**16**). Crystallization from toluene afforded yellowish crystals, yield = 0.3 g, 84%. Mp (°C): 138. IR (KBr): 1722 (C=O), 1631 and 1577 (C=N) cm⁻¹. ¹H NMR (400 MHz, DMSO-*d*₆): 1.61 (d, 3H, *J* 7.2 Hz, CH₃), 1.80 and 1.97 (s, 3H, CH₃), 4.40 (q, 1H, *J* 7.2 Hz, CH), 4.67 (s, 2H, CH₂), 6.73 (d, 2H, *J* 8.0 Hz, Ar), 6.93 (m, 1H, Ar), 7.23 (t, 2H, *J* 7.9 Hz, Ar), 7.38–7.51 (m, 5H, Ar). ¹³C NMR (100 MHz, DMSO-*d*₆): 18.8 and 19.4 (CH₃), 26.2 (CH₃), 41.2 (CH), 64.5 (CH₂), 114.0 (CH, Ar), 121.0 (CH, Ar), 127.9 (CH, Ar), 128.4 (CH, Ar), 128.7 (CH, Ar), 129.6 (CH, Ar), 135.0 (C–N, Ar), 157.6 (C=N), 160.9 (C–O, Ar), 164.4 (S–C=N), 174.6 (C=O). HRMS (ESI): 354.1264 [M + H]⁺. Anal. Calcd for C₁₉H₁₉SO₂N₃: C, 64.57; H, 5.42; N, 11.89; S, 9.07; found: C, 64.50; H, 5.39; S, 10.89; N, 11.80.

2-((1-Phenoxypropan-2-ylidene)hydrazono)-3-phenyl-5-ethylthiazolidin-4-one (**17**). Crystallization from cyclohexane/toluene (1:1) afforded colorless crystals, yield = 0.26 g, 70%. Mp (°C): 118. IR (KBr): 1722 (C=O), 1634 and 1576 (C=N) cm⁻¹. ¹H NMR (400 MHz, DMSO-*d*₆): 1.01 (t, *J* 7.2 Hz, 3H, CH₃), 1.81 (s, 3H, CH₃), 1.89–1.98 (m, 1H, CH₂), 2.03–2.09 (m, 1H, CH₂), 4.38–4.41 (q, 1H, *J* 7.2 and 4.4 Hz, CH), 4.66 (s, 2H, CH₂), 6.92–6.98 (m, 3H, Ar), 7.26–7.30 (m, 2H, Ar), 7.34 and 7.36 (two s, 2H, Ar), 7.41–7.44 (m, 1H, Ar), 7.48–7.51 (m, 2H, Ar). ¹³C NMR (100 MHz, DMSO-*d*₆): 10.1 (CH₃), 14.6 (CH₃), 25.7 (CH₂), 48.1 (CH), 70.6 (CH₂), 114.7 (CH, Ar), 120.9 (CH, Ar), 127.9 (CH, Ar), 128.5 (CH, Ar), 128.8 (CH, Ar), 129.4 (CH, Ar), 134.9 (C–N, Ar), 158.0 (C=N), 161.5 (C–O, Ar), 163.6 (S–C=N), 173.8 (C=O). HRMS (ESI): 368.1422 [M + H]⁺. Anal. Calcd for C₂₀H₂₁SO₂N₃: C, 65.37; H, 5.76; N, 11.44; S, 8.73; found: C, 65.31; H, 5.64; S, 8.07; N, 11.27.

2-((1-Phenoxypropan-2-ylidene)hydrazono)-3-phenyl-5-isopropylthiazolidin-4-one (**18**). Crude was washed with ethyl ether, affording colorless crystals, yield = 0.3 g, 78%. Mp (°C): 128–130. IR (KBr): 1724 (C=O), 1632 and 1579 (C=N) cm⁻¹. ¹H NMR (400 MHz, DMSO-*d*₆): 1.01 (d, 3H, *J* 4.0 Hz, CH₃), 1.08 (d, 3H, *J* 4.0 Hz, CH₃), 1.86 (s, 3H, CH₃), 2.51 (t, 1H, *J* 4.0 and 3.4 Hz, CH), 4.52 (m, 1H, *J* 3.4 Hz, CH), 4.72 (s, 2H, CH₂), 6.97–7.03 (m, 3H, Ar), 7.31–7.38 (m, 4H, Ar), 7.46–7.56 (m, 3H, Ar). ¹³C NMR (100 MHz, DMSO-*d*₆): 14.6 (CH₃), 16.4 (CH₃), 20.1 (CH₃), 30.4 (CH), 53.6 (CH), 70.6 (CH₂), 114.7 (CH, Ar), 120.9 (CH, Ar), 127.8 (CH, Ar), 128.5 (CH, Ar), 128.9 (CH, Ar), 129.4 (CH, Ar), 134.8 (C–N, Ar), 158.0 (C=N), 161.4 (C–O, Ar), 163.8 (S–C=N), 173.4 (C=O). HRMS (ESI): 382.1580 [M + H]⁺. Anal. Calcd for C₂₁H₂₃SO₂N₃: C, 66.12; H, 6.08; N, 11.01; S, 8.41; found: C, 66.48; H, 5.70; S, 6.73; N, 10.81.

2-((1-Phenoxypropan-2-ylidene)hydrazono)-3,5-diphenylthiazolidin-4-one (**19**). Crystallization from cyclohexane afforded colorless crystals, yield = 0.32 g, 74%. Mp (°C): 159. IR (KBr): 1715 (C=O), 1628 and 1590 (C=N) cm⁻¹. ¹H NMR (400 MHz, acetone-*d*₆): 1.01 (d, 3H, *J* 4.0 Hz, CH₃), 1.08 (d, 3H, *J* 4.0 Hz, CH₃), 1.86 (s, 3H, CH₃), 2.51 (t, 1H, *J* 4.0 and 3.4 Hz, CH), 4.52 (m, 1H, *J* 3.4 Hz, CH), 4.72 (s, 2H, CH₂), 6.97–7.03 (m, 3H, Ar), 7.31–7.38 (m, 4H, Ar), 7.46–7.56 (m, 3H, Ar). ¹³C NMR (100 MHz, acetone-*d*₆): 14.6 (CH₃), 16.4 (CH₃), 20.1 (CH₃), 30.4 (CH), 53.6 (CH), 70.6 (CH₂), 114.7 (CH, Ar), 120.9 (CH, Ar), 127.8 (CH, Ar), 128.5 (CH, Ar), 128.9 (CH, Ar), 129.4 (CH, Ar), 134.8 (C–N, Ar), 158.0 (C=N), 161.4 (C–O, Ar), 163.8 (S–C=N), 173.4 (C=O). HRMS (ESI): 416.1433 [M + H]⁺. Anal. Calcd for C₂₄H₂₁SO₂N₃: C, 69.37; H, 5.09; N, 10.11; S, 7.72; found: C, 69.35; H, 5.00; S, 8.01; N, 10.21.

Synthesis of 2-Iminothiazolidine-4-thiones 20 and 21. Example for Compound 21: A solution of 2-iminothiazolidin-4-one **9** (0.34 g, 1.5 mmol) in anhydrous 1,4-dioxane/toluene (1:1, 50 mL) was added to a 100 mL round-bottom flask under magnetic stirring in N₂ and slightly warmed. Then Lawesson's reagent (1.0 g, 2.6 mmol) was added in portions, and the brownish mixture was kept under stirring and heating overnight. After cooling back to rt, the solvent was evaporated to half volume. Water was added and extracted with ethyl ether and then brine. The organic layers were then combined and dried with MgSO₄, and solvent was removed under reduced pressure and then dried over SiO₂. The compound was isolated after column chromatography.

2-((1-Phenoxypropan-2-ylidene)hydrazono)-3,5-diphenylthiazolidin-4-one (**20**). After elution with hexane/ethyl acetate (7:3) to a short silica gel column, yellowish crystals were obtained, yield = 0.2 g, 54%. Mp (°C): 131. IR (KBr): 1620 and 1596 (C=N) cm⁻¹. ¹H NMR (400 MHz, acetone-*d*₆): 1.90 (s, 3H, CH₃), 4.69 (s, 2H, CH₂), 5.40 (s, 1H, CH), 6.91–7.03 (m, 3H, Ar), 7.24–7.30 (m, 2H, Ar), 7.35–7.40 (m, 3H, Ar), 7.42–7.7.56 (m, 6H, Ar). ¹³C NMR (100 MHz, acetone-*d*₆): 27.5 (CH₃), 56.1 (CH), 72.0 (CH₂), 115.2 (CH, Ar), 115.7 (CH, Ar), 121.9 (CH, Ar), 129.01 (CH, Ar), 129.32 (CH, Ar), 129.38 (CH, Ar), 129.72 (CH, Ar), 129.84 (CH, Ar), 130.4 (CH, Ar), 136.6 (C–N, Ar), 138.0 (C–N, Ar), 159.6 (C=N), 162.4 (C–O, Ar), 168.0 (S–C=N), 189.1 (C=S). Anal. Calcd for C₂₄H₂₁S₂O₃N₃: C, 66.79; H, 4.90; N, 9.74; S, 14.86; found: C, 66.81; H, 5.00; S, 15.11; N, 14.01.

2-((1-Phenoxypropan-2-ylidene)hydrazono)-5-ethylthiazolidin-4-thione (**21**). After elution with hexane/ethyl acetate (7:3), yellowish crystals were obtained, yield = 0.28 g, 60%. Mp (°C): 111. IR (KBr): 1620 and 1590 (C=N) cm⁻¹. ¹H NMR (300 MHz, DMSO-*d*₆): 0.92 (t, 3H, *J* 7.5 Hz, CH₃), 1.74–1.82 (m, 1H, CH₂), 1.95–1.98 (m, 1H, CH₂), 2.06 (s, 3H, CH₃), 4.20–4.24 (q, 1H, *J* 4.2 and 7.8 Hz, CH), 4.70 (s, 2H, CH₂), 6.93–7.00 (m, 3H, Ar), 7.26–7.32 (m, 2H, Ar). ¹³C NMR (75.5 MHz, DMSO-*d*₆): 10.3 (CH₃), 14.6 (CH₃), 25.5 (CH₂), 49.0 (CH), 70.8 (CH₂), 114.7 (CH, Ar), 121.0 (CH, Ar), 129.5 (CH, Ar), 158.0 (C=N), 161.9 (C–O, Ar), 163.4 (S–C=N), 188.9 (C=S). Anal. Calcd for C₁₄H₁₇S₂O₃N₃: C, 54.69; H, 5.57; N, 13.67; S, 20.86; found: C, 54.71; H, 5.60; S, 19.99; N, 14.05.

2-((1-Phenoxypropan-2-ylidene)hydrazono)-3-(4-tolyl)-5-ethylthiazolidin-4-one (**22**). Crystallization from cyclohexane/toluene (1:1) afforded colorless crystals, yield = 0.26 g, 68%. Mp (°C): 140. IR (KBr): 1722 (C=O), 1634 and 1575 (C=N) cm⁻¹. ¹H NMR (400 MHz, DMSO-*d*₆): 1.01 (t, *J* 7.2 Hz, 3H, CH₃), 1.81 (s, 3H, CH₃), 1.89–1.98 (m, 1H, CH₂), 2.03–2.09 (m, 1H, CH₂), 2.67 (s, 3H, CH₃) 4.38–4.40

(q, 1H, *J* 7.2 and 4.5 Hz, CH), 4.66 (s, 2H, CH₂), 6.92–6.98 (m, 3H, Ar), 7.20–7.27 (m, 2H, Ar), 7.29 (d, 2H, Ar), 7.60 (d, 2H, Ar). ¹³C NMR (100 MHz, DMSO-*d*₆): 10.1 (CH₃), 14.6 (CH₃), 23.5 (CH₃), 25.7 (CH₂), 48.1 (CH), 70.6 (CH₂), 114.7 (CH, Ar), 120.9 (CH, Ar), 127.9 (CH, Ar), 128.5 (CH, Ar), 129.4 (CH, Ar), 134.9 (C–N, Ar), 158.0 (C=N), 161.5 (C–O, Ar), 163.6 (S–C=N), 174.1 (C=O). Anal. Calcd for C₂₁H₂₃SO₂N₃: C, 66.12; H, 6.08; N, 11.01; S, 8.41; found: C, 66.10; H, 6.01; S, 9.10; N, 11.11.

2-((1-Phenoxypropan-2-ylidene)hydrazono)-3-(4-anisyl)-5-ethylthiazolidin-4-one (**23**). Crystallization from toluene afforded colorless crystals, yield = 0.28 g, 70%. Mp (°C): 162. IR (KBr): 1722 (C=O), 1630 and 1576 (C=N) cm⁻¹. ¹H NMR (400 MHz, DMSO-*d*₆): 1.00 (t, *J* 7.2 Hz, 3H, CH₃), 1.81 (s, 3H, CH₃), 1.89–1.98 (m, 1H, CH₂), 2.02–2.08 (m, 1H, CH₂), 3.82 (s, 3H, OCH₃) 4.38–4.40 (q, 1H, *J* 7.2 and 5 Hz, CH), 4.66 (s, 2H, CH₂), 6.92–6.98 (m, 3H, Ar), 7.20–7.27 (m, 2H, Ar), 7.29 (d, 2H, *J* 9.1 Hz, Ar), 7.69 (d, 2H, *J* 9.1 Hz, Ar). ¹³C NMR (100 MHz, DMSO-*d*₆): 11.0 (CH₃), 14.6 (CH₃), 25.7 (CH₂), 48.1 (CH), 54.0 (CH₃), 63.5 and 70.6 (CH₂), 114.7 (CH, Ar), 120.9 (CH, Ar), 127.9 (CH, Ar), 128.5 (CH, Ar), 129.4 (CH, Ar), 134.9 (C–N, Ar), 155 (C–O, Ar) 157.0 (C=N), 161.5 (C–O, Ar), 163.6 (S–C=N), 174.1 (C=O). Anal. Calcd for C₂₁H₂₃SO₃N₃: C, 63.45; H, 5.83; N, 10.57; S, 8.07; found: C, 63.44; H, 5.91; S, 8.99; N, 10.42.

2-((1-Phenoxypropan-2-ylidene)hydrazono)-3-(cyclohexyl)-5-ethylthiazolidin-4-one (**24**). Crystallization from cyclohexane afforded colorless crystals, yield = 0.26 g, 71%. Mp (°C): 139–141. IR (KBr): 1728 (C=O), 1630 and 1576 (C=N) cm⁻¹. ¹H NMR (400 MHz, DMSO-*d*₆): 1.00 (t, *J* 7.2 Hz, 3H, CH₃), 1.81 (s, 3H, CH₃), 1.89–1.98 (m, 1H, CH₂), 2.02–2.08 (m, 1H, CH₂), 3.82 (s, 3H, OCH₃) 4.38–4.40 (q, 1H, *J* 7.2 and 5 Hz, CH), 4.66 (s, 2H, CH₂), 6.92–6.98 (m, 3H, Ar), 7.20–7.27 (m, 2H, Ar), 7.29 (d, 2H, *J* 9.1 Hz, Ar), 7.69 (d, 2H, *J* 9.1 Hz, Ar). HRMS (ESI): 374.1919 [M + H]⁺. Anal. Calcd for C₂₀H₂₇SO₂N₃: C, 64.31; H, 7.29; N, 11.25; S, 8.58; found: C, 64.31; H, 7.21; N, 11.39; S, 9.00.

General Procedure for the Synthesis of 2-Imino-1,3-thiazoles 26–45. Example for Compound 26: Thiosemicarbazone **4a** (0.24 g, 1 mmol) dissolved in 2-propanol (5 mL) was transferred to a boiling tube and placed in an ultrasound bath (40 MHz, 180 V). Then 2-bromoacetophenone (0.21 g, 1.1 mmol) was added to the mixture and allowed to react until the consumption of the starting materials (30–45 min). The reaction was cooled, and the colorful precipitate was separated in a Büchner funnel with a sintered disc filter, washed with cold propanol followed by cold water, and then dried over SiO₂ in a glass desiccator under vacuum. Pure products were obtained after recrystallization using the solvent system detailed below for each compound.

2-((1-Phenoxypropan-2-ylidene)hydrazinyl)-4-phenyl-1,3-thiazole (**26**). Crystallization from methanol afforded pinkish crystals, yield = 0.25 g, 77%. Mp (°C): 157. IR (KBr): 1618 (C=N), cm⁻¹. ¹H NMR (400 MHz, DMSO-*d*₆): 2.03 (s, 3H, CH₃), 4.63 (s, 2H, CH₂), 6.07 (broad s, 1H, N–H), 6.93–7.01 (m, 3H, 2H Ar and 1H thiazole), 7.27–7.42 (m, 6H, Ar), 7.83–7.86 (m, 2H, Ar). ¹³C NMR and DEPT (100 MHz, DMSO-*d*₆): 14.7 (CH₃), 71.8 (CH₂), 104.5 (CH, thiazole), 115.2 (CH, Ar), 121.4 (CH, Ar), 126.0 (CH, Ar), 128.0 (CH, Ar), 128.2 (CH, Ar), 128.7 (CH, Ar), 129.4 (CH, Ar), 129.9 (Ar), 134.7 (Ar), 148.1 (C=CH, thiazole), 158.1 (C–O), 169.9 (S–C=N). HRMS (ESI): 324.1171 [M + H]⁺. Anal. Calcd for C₁₈H₁₇SON₃: C, 66.85; H, 5.30; N, 12.99; S, 9.91; found: C, 66.52; H, 5.40; N, 13.00; S, 9.71.

2-((1-Phenoxypropan-2-ylidene)hydrazinyl)-4-(2-pyridinyl)-1,3-thiazole (**27**). Crystallization from methanol afforded greenish crystals, yield = 0.24 g, 74%. Mp (°C): 136. IR (KBr): 3364 (N–H), 1620 and 1582 (C=N) cm⁻¹. ¹H NMR (400 MHz, DMSO-*d*₆): 2.05 (s, 3H, CH₃), 4.65 (s, 2H, CH₂), 5.5–6.5 (broad s, 1H, NH), 6.92–7.02 (m, 3H, Ar), 7.27–7.31 (m, 2H, Ar), 7.82 (t, 1H, *J* 8.0 and 9.6 Hz, Ar), 8.14 (s, 1H, CH thiazole), 8.35 (d, 1H, *J* 10 Hz, Ar), 8.46 (t, 1H, *J* 10 Hz, Ar), 8.75 (d, 1H, *J* 8 and 9.6 Hz, Ar). ¹³C NMR and DEPT (100 MHz, DMSO-*d*₆): 13.0 and 14.6 (CH₃), 69.71 and 71.4 (CH₂), 114.4 (CH, thiazole), 114.8 (CH, Ar), 121.0 (CH, Ar), 123.1 (CH, Ar), 124.7 (CH, Ar), 129.5 (CH, Ar), 143.3 (CH, Ar), 143.6 (CH, Ar), 144.8 (CH, Ar), 146.4 (Ar), 149.2 (C=CH, thiazole), 158.0 (C=N), 158.7 (C–O, Ar), 170.0 and 170.6 (S–C=N). HRMS (ESI): 325.1123 [M + H]⁺.

2-((1-Phenoxypropan-2-ylidene)hydrazinyl)-4-(3-pyridinyl)-1,3-thiazole (**28**). Crystallization from methanol afforded greenish crystals, yield = 0.2 g, 61%. Mp (°C): 136. IR (KBr): 1621 and 1586 (C=N) cm⁻¹. ¹H NMR (400 MHz, DMSO-*d*₆): 2.05 (s, 3H, CH₃), 4.64 (s, 2H, CH₂), 5.5–6.5 (broad s, 1H, NH), 6.92–7.02 (m, 3H, Ar), 7.27–7.30 (m, 2H, Ar), 7.82 (t, 1H, *J* 10 Hz, Ar), 8.14 (s, 1H, CH of thiazole), 8.40 (d, 2H, *J* 10 Hz, Ar), 8.46 (t, 1H, *J* 10 Hz, Ar), 8.81 (s, 1H, Ar). ¹³C NMR (100 MHz, DMSO-*d*₆): 14.1 (CH₃), 69.71 and 71.4 (CH₂), 114.4 (CH, thiazole), 114.7 (CH, Ar), 120.9 (CH, Ar), 125.5 (CH, Ar), 129.1 (CH, Ar), 129.4 (CH, Ar), 131.2 (Ar), 137.0 (Ar), 148.2, 149.1 (C=N), 158.0 (C–O, Ar), 169.4 (S–C=N).

2-((1-Phenoxypropan-2-ylidene)hydrazinyl)-4-(4-pyridinyl)-1,3-thiazole (**29**). Crystallization from methanol afforded greenish crystals, yield = 0.23 g, 70%. Mp (°C): 140. IR (KBr): 3339 (N–H), 1617 and 1567 (C=N) cm⁻¹. ¹H NMR (400 MHz, DMSO-*d*₆): 2.03 (s, 3H, CH₃), 4.63 (s, 2H, CH₂), 6.94–7.00 (m, 3H, Ar), 7.28 (broad s, 2H, Ar), 7.28 (d, *J* 9 Hz, 2H, Ar), 7.70 (d, *J* 9 Hz, 2H, Ar), 11.28 (broad s, 1H, NH). ¹³C NMR and DEPT (100 MHz, DMSO-*d*₆): 14.3 (CH₃), 71.2 (CH₂), 114.4 (CH, thiazole), 114.7 (CH, Ar), 120.9 (CH, Ar), 125.5 (CH, Ar), 129.1 (CH, Ar), 129.4 (CH, Ar), 131.2 (Ar), 137.0 (Ar), 148.2, 149.1 (C=N), 158.0 (C–O, Ar), 169.4 (S–C=N).

2-((1-Phenoxypropan-2-ylidene)hydrazinyl)-4-(4-tolyl)-1,3-thiazole (**30**). Crystallization from methanol afforded yellowish crystals, yield = 0.2 g, 60%. Mp (°C): 160. IR (KBr): 1618 (C=N) cm⁻¹. ¹H NMR (400 MHz, DMSO-*d*₆): 2.03 (s, 3H, CH₃), 2.32 (s, 3H, CH₃), 4.63 (s, 2H, CH₂), 6.17 (broad s, 1H, N–H), 6.92–7.00 (m, 3H, Ar), 7.20–7.30 (m, 5H, 4H of Ar and 1H of thiazole), 7.71–7.74 (m, 2H, Ar). ¹³C NMR (100 MHz, DMSO-*d*₆): 14.8 (CH₃), 21.2 (CH₃), 71.6 (CH₂), 103.6 (CH, thiazole), 115.2 (CH, Ar), 121.4 (CH, Ar), 126.0 (CH, Ar), 128.0 (CH, Ar), 128.2 (CH, Ar), 129.3 (CH, Ar), 129.6 (CH, Ar), 129.9 (CH, Ar), 130.1 (Ar), 137.5 (Ar), 158.5 (C–O, Ar), 169.9 (S–C=N). HRMS (ESI): 338.1327 [M + H]⁺. Anal. Calcd for C₁₉H₁₉SON₃: C, 67.63; H, 5.68; N, 12.45; S, 9.50; found: C, 67.60; H, 5.64; N, 12.23; S, 9.40.

2-((1-Phenoxypropan-2-ylidene)hydrazinyl)-4-(4-anisyl)-1,3-thiazole (**31**). Crystallization from ethanol afforded pale greenish crystals, yield = 0.25 g, 70%. Mp (°C): 168. IR (KBr): 1613 and 1601 (C=N) cm⁻¹. ¹H NMR (300 MHz, DMSO-*d*₆): 1.99 and 2.04 (s, 3H, CH₃), 3.76 (s, 3H, OCH₃), 4.64 and 4.90 (s, 2H, CH₂), 6.91–7.01 (m, 5H, Ar), 7.17 (s, 1H, CH of thiazole), 7.24–7.32 (d, 2H, *J* 2.5 Hz, Ar), 7.72–7.81 (d, 2H, *J* 2.5 Hz, Ar), 10.55 (broad s, 1H, N–H). ¹³C NMR and DEPT (75.5 MHz, DMSO-*d*₆): 14.6 (CH₃), 55.2 (OCH₃), 71.1 (CH₂), 102.3 (CH, thiazole), 114.1 (CH, Ar), 113.7 (CH, Ar), 114.8 (CH, Ar), 121.0 (CH, Ar), 125.8 (CH, Ar), 127.1 (CH, Ar), 129.3 (CH, Ar), 129.6 (CH, Ar), 146.8 (CH=C), 149.6 (C=N), 158.1 (C–O, Ar), 159.2 (C–O, Ar), 169.5 (S–C=N). HRMS (ESI): 354.1282 [M + H]⁺. Anal. Calcd for C₁₉H₁₉SO₂N₃: C, 64.57; H, 5.42; N, 11.89; S, 9.07; found: C, 64.60; H, 5.35; N, 11.80; S, 8.91.

2-((1-Phenoxypropan-2-ylidene)hydrazinyl)-4-(4-fluorophenyl)-1,3-thiazole (**32**). Off-white crystals, yield = 0.29 g, 85%. Mp (°C): 157. IR (KBr): 1619 and 1608 (C=N) cm⁻¹. ¹H NMR (300 MHz, DMSO-*d*₆): 1.98 and 2.03 (s, 3H, CH₃), 4.59 and 4.62 (s, 2H, CH₂), 6.89–6.97 (m, 3H, Ar), 7.20–7.30 (m, 5H, 4H of Ar and 1CH of thiazole), 7.82–7.87 (m, 2H, Ar), 10.53 (broad s, 1H, N–H). After addition of D₂O, the signal at δ 10.53 ppm decreased. ¹³C NMR (75.5 MHz, DMSO-*d*₆): 14.7 (CH₃), 71.2 (CH₂), 104.3 (CH, thiazole), 114.5 (CH, Ar), 114.8 (CH, Ar), 115.2 (CH, Ar), 121.1 (CH, Ar), 127.8 (CH, Ar), 127.9 (CH, Ar), 129.6 (CH, Ar), 129.8 (C–F), 130.0 (C–F), 146.7 (Ar), 146.9 (CH=C), 148.5 (C=N), 158.1 (C–O), 169.4 and 169.7 (S–C=N). HRMS (ESI): 342.1099 [M + H]⁺. Anal. Calcd for C₁₈H₁₆SOFN₃: C, 63.32; H, 4.72; N, 12.31; S, 9.39; found: C, 63.40; H, 4.69; N, 12.30; S, 9.22.

2-((1-Phenoxypropan-2-ylidene)hydrazinyl)-4-(4-chlorophenyl)-1,3-thiazole (**33**). Crystallization from ethanol afforded reddish crystals, yield = 0.26 g, 72%. Mp (°C): 164–165. IR (KBr): 1620 and 1586 (C=N) cm⁻¹. ¹H NMR (300 MHz, DMSO-*d*₆): 2.09 (s, 3H, CH₃), 4.63 and 4.90 (s, 2H, CH₂), 6.90–7.00 (m, 3H, Ar), 7.25–7.46 (m, 5H, 4H of Ar and 1CH of thiazole), 7.80–7.85 (d, 2H, *J* 7.8 Hz, Ar), 10.61 (broad s, 1H, N–H). ¹³C NMR (75.5 MHz, DMSO-*d*₆): 14.6 (CH₃), 71.2 (CH₂), 104.4 (CH, thiazole), 114.8 (CH, Ar), 121.0 (CH, Ar),

125.7 (CH, Ar), 127.4 (CH, Ar), 127.9 (CH, Ar), 128.0 (CH, Ar), 128.4 (CH, Ar), 128.6 (CH, Ar), 129.6 (CH, Ar), 133.3 (Ar), 148.3 (CH=C), 149.4 (C=N), 158.1 (C-O, Ar), 169.6 (S-C=N). HRMS (ESI): 358.0909 [M + H]⁺. Anal. Calcd for C₁₈H₁₆SOClN₃: C, 60.41; H, 4.51; N, 11.74; S, 8.96; found: C, 61.01; H, 4.62; N, 12.03; S, 8.81.

2-((1-Phenoxypropan-2-ylidene)hydrazinyl)-4-(4-bromophenyl)-1,3-thiazole (34). Brownish crystals, yield = 0.8 g, 66%. Mp (°C): 171. IR (KBr): 3317 (N-H), 1615 and 1572 (C=N) cm⁻¹. ¹H NMR (400 MHz, DMSO-*d*₆): 2.02 (s, 3H, CH₃), 4.62 (s, 2H, CH₂), 6.92–7.01 (m, 3H, Ar), 7.26–7.35 (m, 2H, Ar), 7.35 (s, 1H, CH thiazole), 7.58 (d, 2H, J 7.5 Hz, Ar), 7.80 (d, 2H, J 7.5 Hz, Ar), 11.10 (s, 1H, N-H). ¹³C NMR (100 MHz, DMSO-*d*₆): 14.2 (CH₃), 71.3 (CH₂), 104.8, 114.7 (CH, Ar), 120.4 (CH, Ar), 120.9 (CH, Ar), 127.4 (CH, Ar), 129.4 (CH, Ar), 131.4 (CH, Ar), 133.9 (Ar), 147.1 (C=C, thiazole), 149.3 (C=N), 158.1 (C-O, Ar), 169.6 (S-C=N). HRMS (ESI): 402.0272 [M + H]⁺. Anal. Calcd for C₁₈H₁₆SOBrN₃: C, 53.74; H, 4.01; N, 10.44; S, 7.97; found: C, 53.72; H, 4.02; N, 10.55; S, 7.57.

2-((1-Phenoxypropan-2-ylidene)hydrazinyl)-4-(4-nitrophenyl)-1,3-thiazole (35). Crystallization from 2-propanol afforded yellowish crystals, yield = 0.3 g, 80%. Mp (°C): 171–173. IR (KBr): 3337 (N-H), 1598 and 1565 (C=N) cm⁻¹. ¹H NMR (300 MHz, DMSO-*d*₆): 2.03 (s, 3H, CH₃), 4.63 (s, 2H, CH₂), 6.92–7.01 (m, 3H, Ar), 7.29 (t, 2H, Ar), 7.70 (s, 1H, CH of thiazole), 8.07 (d, 2H, J 8.7 Hz, Ar), 8.29 (d, 2H, J 9.0 Hz, Ar), 11.26 (s, 1H, N-H). ¹³C NMR (75.5 MHz, DMSO-*d*₆): 14.3 (CH₃), 71.3 (CH₂), 108.9 (CH, thiazole), 114.8 (CH, Ar), 121.0 (CH, Ar), 124.1 (CH, Ar), 126.3 (CH, Ar), 129.5 (CH, Ar), 140.7 (CH, Ar), 146.1 (Ar), 147.6 (CH=C), 148.5 (C=N), 158.1 (C-O), 169.9 (S-C=N). HRMS (ESI): 369.1072 [M + H]⁺.

2-((1-Phenoxypropan-2-ylidene)hydrazinyl)-4-(3-nitrophenyl)-1,3-thiazole (36). Crystallization from toluene afforded yellowish crystals, yield = 0.18 g, 48%. Mp (°C): 159–160. IR (KBr): 3337 (N-H), 1598 and 1565 (C=N) cm⁻¹. ¹H NMR (400 MHz, DMSO-*d*₆): 2.64 (s, 3H, CH₃), 5.15 (s, 2H, CH₂), 7.40 (t, 1H, Ar), 7.49 (d, 2H, Ar), 7.75 (t, 2H, Ar), 7.89 (s, 1H, CH of thiazole), 8.10 (t, 1H, J 8.0 Hz, Ar), 8.56 (d, 1H, J 8.0 Hz, Ar), 8.70 (d, 1H, J 8.0 Hz, Ar), 10.58 (broad s, 1H, N-H). ¹³C NMR and DEPT (100 MHz, DMSO-*d*₆): 23.5 (CH₃), 82.0 (CH₂), 116.7 (CH, thiazole), 125.4 (CH, Ar), 130.8 (CH, Ar), 131.5 (CH, Ar), 132.3 (CH, Ar), 139.9 (CH, Ar), 140.3 (CH, Ar), 141.8 (Ar), 147.3 (Ar), 157.8 (CH=C), 159.3 (C=N), 169.2 (C-O, Ar), 180.1 (S-C=N). HRMS (ESI): 369.1042 [M + H]⁺.

2-((1-Phenoxypropan-2-ylidene)hydrazinyl)-4-(3,4-dichlorophenyl)-1,3-thiazole (37). Crystallization from methanol afforded reddish crystals, yield = 0.26 g, 66%. Mp (°C): 160. IR (KBr): 3338 (N-H), 1615 and 1565 (C=N) cm⁻¹. ¹H NMR (400 MHz, DMSO-*d*₆): 2.01 (s, 3H, CH₃), 4.61 (s, 2H, CH₂), 6.92–7.00 (m, 3H, Ar), 7.26–7.30 (m, 3H, Ar), 7.50 (s, 1H, 1H thiazole), 7.64 (d, 1H, J 8 Hz, Ar), 7.82 (d, 1H, J 8 Hz, Ar), 8.07 (s, 1H, Ar), 11.10 (broad s, 1H, N-H). ¹³C NMR and DEPT (100 MHz, DMSO-*d*₆): 14.2 (CH₃), 71.3 (CH₂), 106.2 (CH, thiazole), 114.7 (CH, Ar), 120.9 (CH, Ar), 125.5 (CH, Ar), 127.1 (CH, Ar), 129.4 (CH, Ar), 129.6 (CH, Ar), 130.8 (CH, Ar), 131.4 (Ar), 135.2 (Ar), 147.5 (CH=C), 147.7 (C=N), 158.1 (C-O, Ar), 169.7 (S-C=N). HRMS (ESI): 392.0378 [M + H]⁺.

2-((1-Phenoxypropan-2-ylidene)hydrazinyl)-4-(2,4-dichlorophenyl)-1,3-thiazole (38). Crystallization from methanol afforded reddish crystals, yield = 0.17 g, 55%. Mp (°C): 200. IR (KBr): 1568 (C=N) cm⁻¹. ¹H NMR (400 MHz, DMSO-*d*₆): 2.01 (s, 3H, CH₃), 4.63 (s, 2H, CH₂), 6.92–7.00 (m, 3H, Ar), 7.26–7.30 (m, 2H, Ar), 7.36 (s, 1H, CH of thiazole), 7.47–7.49 (d, 1H, J 8.4 Hz, Ar), 7.66 (s, 1H, Ar), 7.89 (d, 1H, J 8.4 Hz, Ar), 11.25 (broad s, 1H, N-H). ¹³C NMR (100 MHz, DMSO-*d*₆): 14.2 (CH₃), 71.3 (CH₂), 109.4 (CH, thiazole), 114.8 (CH, Ar), 120.9 (CH, Ar), 127.4 (CH, Ar), 129.4 (CH, Ar), 129.6 (CH, Ar), 131.5 (CH, Ar), 132.1 (CH, Ar), 132.2 (CH, Ar), 132.3 (Ar), 135.2 (Ar), 145.8 (CH=C), 147.2 (C=N), 158.1 (C-O, Ar), 168.6 (S-C=N). HRMS (ESI): 392.0378 [M + H]⁺.

2-((1-Phenoxypropan-2-ylidene)hydrazinyl)-4-(2,3,4-trichlorophenyl)-1,3-thiazole (39). Crystallization from toluene afforded reddish crystals, yield = 0.24 g, 50%. Mp (°C): 200 (decomp). IR (KBr): 3321 (N-H), 1615 and 1565 (C=N) cm⁻¹. ¹H NMR (300 MHz, DMSO-*d*₆): 2.01 (s, 3H, CH₃), 4.63 (s, 2H, CH₂), 6.92–7.01 (m, 3H, Ar), 7.29 (t, 2H, Ar), 7.40 (s, 1H, CH of thiazole), 7.72 (d, 1H, J 8.5 Hz, Ar),

7.81 (d, 1H, J 8.4 Hz, Ar), 11.17 (broad s, 1H, N-H). ¹³C NMR (75.5 MHz, DMSO-*d*₆): 14.2 (CH₃), 71.3 (CH₂), 110.2 (CH, thiazole), 114.8 (CH, Ar), 120.9 (CH, Ar), 128.7 (CH, Ar), 129.4 (CH, Ar), 129.9 (CH, Ar), 130.7 (Ar), 131.1 (Ar), 131.7 (Ar), 134.3 (Ar), 145.9 (CH=C), 147.3 (Ar), 158.1 (C-O), 168.7 (S-C=N). HRMS (ESI): 426.7810 [M + H]⁺.

2-((1-Phenoxypropan-2-ylidene)hydrazinyl)-4-(tert-butylphenyl)-1,3-thiazole (40). Crystallization from toluene afforded yellowish crystals, yield = 0.3 g, 79%. Mp (°C): 180–182. IR (KBr): 1610 and 1586 (C=N) cm⁻¹. ¹H NMR (300 MHz, DMSO-*d*₆): 1.23 (broad s, 9H, 3xCH₃), 2.00 (s, 3H, CH₃), 4.89 (s, 2H, CH₂), 6.92–7.00 (m, 3H, Ar), 7.16–7.20 (d, 2H, J 7.1 Hz, Ar), 7.37–7.42 (m, 3H, 2H Ar, J 7.1 Hz, and 1H of thiazole), 7.48–7.52 (m, 2H, Ar), 10.91 (broad s, 1H, N-H). ¹³C NMR (75.5 MHz, DMSO-*d*₆): 14.2 (CH₃), 31.1 (CH₃), 32.8 (CCH₃), 71.6 (CH₂), 103.6 (CH, thiazole), 115.2 (CH, Ar), 121.4 (CH, Ar), 126.0 (CH, Ar), 128.1 (CH, Ar), 128.2 (CH, Ar), 129.1 (CH, Ar), 129.2 (CH, Ar), 129.9 (Ar), 130.1 (Ar), 135.5 (Ar), 149.1 (C=N), 158.5 (C-O, Ar), 169.9 (S-C=N).

2-((1-Phenoxypropan-2-ylidene)hydrazinyl)-4-(2-naphthalenyl)-1,3-thiazole (41). Crystallization from toluene afforded brownish crystals, yield = 0.26 g, 70%. Mp (°C): 180–182 (decomp). IR (KBr): 1614 and 1490 (C=N) cm⁻¹. ¹H NMR (400 MHz, DMSO-*d*₆): 2.05 (s, 3H, CH₃), 4.64 (s, 2H, CH₂), 6.95–7.02 (m, 3H, Ar), 7.30 (s, 2H, 1H of Ar and 1H of thiazole), 7.47 (d, 3H, Ar), 7.91–8.01 (m, 4H, Ar), 8.39 (s, 1H, Ar), 11.14 (broad s, 1H, N-H). ¹³C NMR and DEPT (100 MHz, DMSO-*d*₆): 14.2 (CH₃), 71.4 (CH₂), 104.7 (CH, thiazole), 114.7 (CH, Ar), 120.9 (CH, Ar), 123.9 (CH, Ar), 124.0 (CH, Ar), 125.9 (CH, Ar), 126.3 (CH, Ar), 127.5 (CH, Ar), 128.0 (CH, Ar), 128.0 (CH, Ar), 129.4 (CH, Ar), 132.1 (CH, Ar), 132.3 (CH, Ar), 138.1 (Ar), 147.1 (CH=C), 158.1 (C-O, Ar), 169.5 (S-C=N). HRMS (ESI): 374.1270 [M + H]⁺. Anal. Calcd for C₂₂H₁₉SON₃: C, 70.75; H, 5.13; N, 11.25; S, 8.59; found: C, 70.68; H, 5.10; N, 11.27; S, 8.62.

2-((1-Phenoxypropan-2-ylidene)hydrazinyl)-4-(2-furanyl)-1,3-thiazole (42). Crystallization from methanol afforded brownish crystals, yield = 0.15 g, 50%. Mp (°C): 210. IR (KBr): 1600 and 1576 (C=N) cm⁻¹. ¹H NMR (400 MHz, DMSO-*d*₆): 2.02 (s, 3H, CH₃), 4.61 (s, 2H, CH₂), 6.58 (two s, 2H, Ar and CH thiazole), 7.00 (broad s, 4H Ar), 7.25 (d, 2H, Ar), 7.67 (s, 1H, Ar), 11.21 (s, 1H, N-H). ¹³C NMR and DEPT (100 MHz, DMSO-*d*₆): 14.2 (CH₃), 71.3 (CH₂), 102.9 (CH, thiazole), 106.0 (CH, Ar), 111.6 (CH, Ar), 114.7 (CH, Ar), 120.9 (CH, Ar), 129.5 (CH, Ar), 142.4 (CH, Ar), 147.2 (C-O, Ar), 150.3 (C=N), 158.1 (C-O, Ar), 170.0 (S-C=N).

2-((1-Phenoxypropan-2-ylidene)hydrazinyl)-4-(2-thiophenyl)-1,3-thiazole (43). Crystallization from methanol afforded brownish crystals, yield = 0.15 g, 53%. Mp (°C): 190–191. IR (KBr): 1620 and 1590 (C=N) cm⁻¹. ¹H NMR (400 MHz, DMSO-*d*₆): 2.02 (s, 3H, CH₃), 4.61 (s, 2H, CH₂), 6.58 (two s, 2H, Ar and CH thiazole), 7.00 (broad s, 4H Ar), 7.25 (d, 2H, Ar), 7.67 (s, 1H, Ar), 10.53 (s, 1H, N-H). ¹³C NMR (100 MHz, DMSO-*d*₆): 14.2 (CH₃), 71.3 (CH₂), 104.0 (CH, thiazole), 106.0 (CH, Ar), 111.6 (CH, Ar), 114.7 (CH, Ar), 120.9 (CH, Ar), 129.5 (CH, Ar), 141.3 (CH, Ar), 142.4 (CH, Ar), 147.2 (C-O, Ar), 150.3 (C=N), 158.1 (C-O, Ar), 170.0 (S-C=N).

2-((1-Phenoxypropan-2-ylidene)hydrazinyl)-3-methyl-4-phenyl-1,3-thiazole (44). Prepared from thiosemicarbazone 4b, crystallization from toluene afforded yellowish crystals, yield = 0.25 g, 73%. Mp (°C): 135. IR (KBr): 1591 (C=N) cm⁻¹. ¹H NMR (300 MHz, DMSO-*d*₆): 2.03 and 2.16 (s, 3H, CH₃), 3.47 (s, 3H, N-CH₃), 4.76 and 5.07 (s, 2H, CH₂), 6.91–6.99 (m, 3H, Ar), 7.02 (s, 1H, S-CH), 7.25–7.31 (m, 2H, Ar), 7.52 (m, 6H, Ar). ¹³C NMR (75.5 MHz, DMSO-*d*₆): 15.4 (CH₃), 35.4 (N-CH₃), 70.6 (CH₂), 114.3, 114.8, 121.0 (Ar), 128.9 (Ar), 129.1, 129.2, 129.5, 129.7, 129.8, 141.8 (CH=C), 158.0 (C=N), 158.7 (C-O, Ar), 169.6 (S-C=N). HRMS (ESI): 338.1326 [M + H]⁺. Anal. Calcd for C₁₉H₁₉SON₃: C, 67.63; H, 5.68; N, 12.45; S, 9.50; found: C, 67.70; H, 5.80; N, 12.53; S, 9.31.

2-((1-Phenoxypropan-2-ylidene)hydrazinyl)-3,4-diphenyl-1,3-thiazole (45). Prepared from thiosemicarbazone 4c, isolated as yellowish crystals, yield = 0.3 g, 75%. Mp (°C): 136. IR (KBr): 1622 and 1591 (C=N) cm⁻¹. ¹H NMR (400 MHz, DMSO-*d*₆): 1.84 (s, 3H, CH₃), 4.63 (s, 2H, CH₂), 6.58 (s, 1H, CH thiazole), 6.92–7.00 (m, 3H, Ar), 7.15 (d, 2H, Ar), 7.22–7.35 (m, 10H, Ar). ¹³C NMR (100 MHz,

DMSO-*d*₆): 14.6 (CH₃), 71.2 (CH₂), 101.3 (CH, thiazole), 114.7 (CH, Ar), 120.7 (CH, Ar), 127.5 (CH, Ar), 128.0 (CH, Ar), 128.20 (CH, Ar), 128.28 (CH, Ar), 128.3 (CH, Ar), 128.6 (CH, Ar), 129.4 (CH, Ar), 130.8 (Ar), 137.6 (Ar), 139.3 (C=CH), 156.9 (C=N), 158.2 (C–O, Ar), 168.6 (S–C=N). Anal. Calcd for C₂₄H₂₁SON₃: C, 72.15; H, 5.30; N, 10.52; S, 8.03; found: C, 72.14; H, 5.31; N, 10.42; S, 7.93.

Molecular Modeling. The optimized structures of all compounds were obtained by using the RM1⁴⁵ method, available as part of the SPARTAN '08 program,⁴⁶ using internal default settings for convergence criteria. Some of these new molecules were synthesized as racemic mixtures, so the molecular modeling treated the two isomers (R and S) independently, when appropriate, and the docking procedure used both isomers for each compound. Docking calculations and analysis were carried using the *T. cruzi* cruzain (PDB ID code: 3IUT) as the target,²³ in which there was a cocrystallized complex with inhibitor **54** (referred to as "KB2"). The active site was defined as all atoms within a radius of 6.0 Å from the cocrystallized ligand. The residues GLN19, CYS25, SER61, LEU67, MET68, ASN70, ASP161, HIS162, TRP184, and GLU208 were treated as flexible, using the conformation library for each one. The GOLD 5.1 program⁴⁷ was used for docking calculations, followed by the Binana program,⁴⁸ which was used to analyze the molecular interactions present in the best docking solutions, using the default setting, except for hydrogen bond distance, which was changed to a maximum of 3.5 Å. Figures were generated with Pymol.⁴⁹

Cruzain Inhibition. Recombinant cruzain was dissolved in acetate buffer (0.1 M; pH 5.5) to a concentration of 0.1 μM. Ten microliters of cruzain in DTT (5 mM) was distributed into a 96-well plate, and 150 μL of the test inhibitor (previously dissolved in DMSO) in phosphate buffer (in the presence of 0.001% EDTA, 100 mM NaCl, and DTT) was added to the respective wells. The plate was incubated at room temperature for 10 min. After this time, 340 μL of a solution containing the protease substrate Cbz-Phe-Arg-7-aminomethylcoumarin (Z-FR-AMC, Sigma-Aldrich Co., St. Louis, MO) was added to each well and the plate incubated. The plate was read 1, 5, and 10 min after the addition of the substrate (concentration of protein and substrate in the reaction was 0.5 nM and 2 μM, respectively). The percentage of cruzain inhibition was calculated using the following equation: $100 - (A_1/A \times 100)$, where *A*₁ means the RFU of the cruzain in the presence of the test inhibitor, and *A* means the RFU for the control well (cruzain plus substrate; no test inhibitor). Each test inhibitor concentration was measured in duplicate, and the IC₅₀ values were estimated employing nonlinear regression from at least nine different concentrations.

Cathepsins L and S Inhibition. Recombinant cathepsin L was dissolved in acetate buffer (0.1 M; pH 5.5) and activated with 1 mM of DTT. Test inhibitors were dissolved in DMSO and then diluted with phosphate buffer containing BSA (0.1%) and EDTA (1 mM) in 0.001% Tween. Protease substrate (Cbz-Phe-Arg-*p*-nitroanilide hydrochloride; denoted ZFR-pNA) in DMSO was suspended in phosphate buffer. Reactions were performed in 24-well plates. First, 90 μL of test inhibitor was distributed into the respective well, followed by the addition of 10 μL of cathepsin L. The plate was incubated for 45 min at room temperature. Then 100 μL of protease substrate was added, and the reaction was incubated for 5 min. The concentration of the protein in the reaction was 30 nM, and the concentration of the substrate was 5.0 μM. IC₅₀ values were calculated as described for cruzain. The same experiment was carried out for cathepsin S.

Animals. Female BALB/c mice (6–8 weeks old) were supplied by the animal breeding facility at Centro de Pesquisas Gonçalo Moniz (Fundação Oswaldo Cruz, Bahia, Brazil) and Centro de Pesquisas Aggeu Magalhães (Fundação Oswaldo Cruz, Pernambuco, Brazil) and maintained in sterilized cages under a controlled environment, receiving a balanced diet for rodents and water ad libitum. All experiments were carried out in accordance with the recommendations from Ethical Issues Guidelines and were approved by the local Animal Ethics Committee.

Parasites. Epimastigotes of *T. cruzi* (Y strain) were maintained at 26 °C in LIT medium (liver infusion tryptose) supplemented with 10% fetal bovine serum (FBS) (Cultilab, Brazil), 1% hemin (Sigma Co., St. Louis, MO), 1% R9 medium (Sigma Co), and 50 μg/mL gentamycin (Novafarma, Brazil). Bloodstream trypomastigote forms of *T. cruzi* were obtained from the supernatant of LLC-MK2 cells previously infected

and maintained in RPMI-1640 medium (Sigma Co.) supplemented with 10% FBS and 50 μg/mL gentamycin at 37 °C and 5% CO₂.

Toxicity to Mouse Splenocytes. Splenocytes from BALB/c mice were placed into 96-well plates at a cell density of 5×10^6 cells/well in RPMI-1640 medium supplemented with 10% of FBS and 50 μg mL⁻¹ of gentamycin. Each test inhibitor was used in at least three concentrations (1.0, 10, and 100 μg mL⁻¹) in triplicate. To each well, an aliquot of test inhibitor suspended in DMSO was added. Negative (untreated) and positive (saponin) controls were used with every plate. The plate was incubated for 24 h at 37 °C and 5% CO₂. After incubation, 1.0 μCi of ³H-thymidine (Perkin-Elmer, Waltham, MA) was added to each well, and the plate was returned to the incubator. The plate was then transferred to a β-radiation counter (Multilabel Reader, Finland), and the percent of ³H-thymidine was determined. Cell viability was measured as the percent of ³H-thymidine incorporation for treated cells in comparison to untreated cells. The highest nontoxic concentration was estimated.

Antiproliferative Activity for Splenocytes. BALB/c mouse splenocytes were placed into 96-well plates at a cell density of 5×10^6 cells/well in RPMI-1640 medium supplemented with 10% of FBS and 100 μg mL⁻¹ of gentamycin. Then 2.0 μg/mL of concanavalin A (con A) suspended in HEPES buffer and test inhibitors **5** and **18** (suspended in DMSO) were added to each well. Controls include untreated plus con A, without con A, and con A plus 0.01 μg/mL of cyclosporin A. Each concentration was assayed in triplicate. The plate was incubated for 72 h at 37 °C and 5% CO₂. According to manufacturer's recommendations, AlamarBlue was added and the plate was incubated for 1 h until AlamarBlue reduction by the living cells to the red fluorescent dye resorufin. After excitation at 530 nm and fluorescence at 590 nm, the signal was measured using a fluorescence microplate reader. Counts of untreated plus con A wells were subtracted from counts of untreated without con A wells. Inhibition (%) of cell proliferation was calculated in comparison to untreated cells. The concentration that results in 50% inhibition of cell proliferation (IC₅₀) was calculated from six different concentrations using nonlinear regression (Origin software).

Antiproliferative Activity for Epimastigotes. Epimastigotes were counted in a hemocytometer and then dispensed into 96-well plates at a cell density of 10⁶ cells/well. Test inhibitors, dissolved in DMSO, were diluted to five different concentrations (1.23, 3.70, 11.11, 33.33, and 100 μg/mL) and added to respective wells in triplicate. The plate was incubated for 11 days at 26 °C, aliquots of each well were collected, and the number of viable parasites were counted in a Neubauer chamber and compared to untreated parasite culture. IC₅₀s were calculated using nonlinear regression on Prism 4.0 GraphPad software. Two independent experiments were carried out; benznidazole (LAFEPE, Brazil) and nifurtimox (Lampit, Roche) were used as the reference inhibitors.

Toxicity for Y Strain Trypomastigotes. Trypomastigotes collected from the supernatant of LLC-MK2 cells were dispensed into 96-well plates at a cell density of 4×10^5 cells/well. Test inhibitors, dissolved in DMSO, were diluted to five different concentrations and added into their respective wells, and the plate was incubated for 24 h at 37 °C and 5% of CO₂. Aliquots of each well were collected, and the number of viable parasites, based on parasite motility, was assessed in a Neubauer chamber. The percentage of inhibition was calculated in relation to untreated cultures. IC₅₀ calculation was also carried out using nonlinear regression with Prism 4.0 GraphPad software. Benznidazole and nifurtimox were used as the reference drugs.

Intracellular Parasite Development. Peritoneal exudate macrophages were seeded at a cell density of 2×10^5 cells/well in a 24-well plate with rounded coverslips on the bottom in RPMI supplemented with 10% FBS and incubated for 24 h. Cells were then infected with Y strain trypomastigotes at a ratio of 10 parasites per macrophage for 2 h. Free trypomastigotes were removed by successive washes using saline solution. Each test inhibitor was dissolved in DMSO at 10 μM and incubated for 6 h. The medium was replaced by a fresh medium, and the plate was incubated for 4 days. Cells were fixed in methanol, and the percentage of infected macrophages and the mean number of amastigotes/infected macrophages were determined by manual counting after Giemsa staining under an optical microscope (Olympus, Tokyo, Japan).

The percentage of infected macrophages and the number of amastigotes per macrophage were determined by counting 100 cells per slide. To estimate the IC_{50} values, compounds were tested in triplicate at 1.0, 10, 25, and 50 μ M.

Trypomastigote Invasion. Peritoneal macrophages (10^5 cells) were plated onto 13-mm glass coverslips in a 24-well plate and allowed to stand for 24 h. The plate was washed with saline solution, and then trypomastigotes were added at a cell density of 1.25×10^7 along with the addition of test inhibitor (at 50 μ M). Amphotericin B (50 μ M) was used as reference inhibitor. The plate was incubated for 2 h at 37 °C and 5% CO_2 , followed by five washes with saline solution to remove extracellular trypomastigotes. Plates were maintained in RPMI medium supplemented with 10% FBS at 37 °C for 2 h. The number of infected cells was counted with optical microscopy using a standard Giemsa staining.

Infection in Mice. Female BALB/c mice (6–8 weeks old) were infected with bloodstream trypomastigotes by intraperitoneal injection of 10^4 parasites in 100 μ L of saline solution. Mice were then randomly divided into groups (six mice per group). After day 5 of postinfection, treatment with 250 μ mol/kg weight of drug **18** was given orally by gavage once a day for five consecutive days. For the control group, benznidazole was also given orally at a dose of 250 μ mol/kg weight. Infection was monitored daily by counting the number of motile parasites in 5 μ L of fresh blood sample drawn from the lateral tail veins as recommended by standard protocols.³⁶

Statistical Analyses. To determine the statistical significance of each group in the in vitro/in vivo experiments of infection, the one-way ANOVA test and the Bonferroni for multiple comparisons were used. A *P* value <0.05 was considered significant. The data are representative of at least two experiments.

■ ASSOCIATED CONTENT

● Supporting Information

NMR, IR, and HRMS spectral data for intermediate compounds, and details for the electron microscopy studies and pharmacological tests. This material is available free of charge via the Internet at <http://pubs.acs.org>. Crystallographic data for compounds **2**, **4**, and **12** can be obtained free of charge from the Cambridge Crystallographic Data Centre (deposition numbers 874915, 874916, and 897962, respectively, www.ccdc.cam.ac.uk/data_request/cif).

■ AUTHOR INFORMATION

Corresponding Author

*Phone: +55 81-21268511, fax: +55 81-21268510; e-mail: diogollucio@gmail.com.

Notes

The authors declare no competing financial interest.

■ ACKNOWLEDGMENTS

This work received support from CNPq (grant 471461/2011-3 to A.C.L.L.), CAPES (grant 23038.003155/2011-37 to V.R.A.P.), FAPESB (PRONEX grant to M.B.P.S.), and European Union ChemBioFight (grant reference 269301 to M.B.P.S.). D.R.M.M. received a CNPq doctoral scholarship and a CAPES-Fulbright Foundation exchange doctoral sponsorship. A.C.L.L., C.A.S., and M.B.P.S. hold a CNPq senior fellowship. The authors acknowledge Prof. James McKerrow for providing recombinant cruzain and plasmid. C.A.S. also thanks the Instituto de Física de São Carlos (University of São Paulo, Brazil) for allowing the use of a Kappa CCD diffractometer.

■ REFERENCES

(1) World Health Organization. Fact sheet no. 340, June 2010. <http://www.who.int/mediacentre/factsheets/fs340/en/index.html> (accessed June 1, 2012).

(2) Rassi, A., Jr.; Rassi, A.; Marin-Neto, J. A. Chagas Disease. *Lancet* **2010**, *375*, 1388–402.

(3) Barrett, M. P.; Burchmore, R. J.; Stich, A.; Lazzari, J. O.; Frasch, A. C.; Cazzulo, J. J.; Krishna, S. The Trypanosomiasis. *Lancet* **2003**, *362*, 1469–1480.

(4) Marin-Neto, J. A.; Rassi, A., Jr.; Avezum, A., Jr.; Mattos, A. C.; Rassi, A. The BENEFIT Trial: Testing the Hypothesis That Trypanocidal Therapy is Beneficial for Patients with Chronic Chagas Heart Disease. *Mem. Inst. Oswaldo Cruz* **2009**, *104*, 319–324.

(5) Marin-Neto, J. A.; Rassi, A., Jr.; Morillo, C. A.; Avezum, A.; Connolly, S. J.; Sosa-Estani, S.; Rosas, F.; Yusuf, S. BENEFIT Investigators. Rationale and Design of a Randomized Placebo-Controlled Trial Assessing the Effects of Etiologic Treatment in Chagas' Cardiomyopathy: The BENznidazole Evaluation For Interrupting Trypanosomiasis (BENEFIT). *Am. Heart J.* **2008**, *156*, 37–43.

(6) Pinazo, M. J.; Muñoz, J.; Posada, E.; López-Chejade, P.; Gállego, M.; Ayala, E.; del Cacho, E.; Soy, D.; Gascon, J. Tolerance of Benznidazole in Treatment of Chagas' Disease in Adults. *Antimicrob. Agents Chemother.* **2010**, *54*, 4896–4899.

(7) Sajid, M.; Robertson, S. A.; Brinen, L. S.; McKerrow, J. H. Cruzain: the Path From Target Validation to the Clinic. In *Advances in Experimental Medicine and Biology, Proteases of Pathogenic Organisms*; Robinson, M. W.; Dalton, J. P., Eds.; Springer Science Business Media, LLC: New York, 2011; vol. 712, pp 100–115.

(8) Duschak, V. G.; Ciaccio, M.; Nassert, J. R.; Basombrio, M. A. Enzymatic Activity, Protein Expression, and Gene Sequence of Cruzain in Virulent and Attenuated *Trypanosoma cruzi* Strains. *J. Parasitol.* **2001**, *87*, 1016–1022.

(9) Doyle, P. S.; Zhou, Y. M.; Hsieh, I.; Greenbaum, D. C.; McKerrow, J. H.; Engel, J. C. The *Trypanosoma cruzi* Protease Cruzain Mediates Immune Evasion. *Plos Pathog.* **2011**, *7*, e1002139.

(10) Aoki, M. P.; Cano, R. C.; Pellegrini, A. V.; Tanos, T.; Guinázú, N. L.; Coso, O. A.; Gea, S. Different Signaling Pathways Are Involved in Cardiomyocyte Survival Induced by a *Trypanosoma cruzi* Glycoprotein. *Microbes Infect.* **2006**, *8*, 1723–1731.

(11) Monteiro, A. C.; Schmitz, V.; Svensjo, E.; Gazzinelli, R. T.; Almeida, I. C.; Todorov, A.; de Arruda, L. B.; Torrecilhas, A. C.; Pesquero, J. B.; Morrot, A.; Bouskela, E.; Bonomo, A.; Lima, A. P.; Müller-Esterl, W.; Scharfstein, J. Cooperative Activation of TLR2 and Bradykinin B2 Receptor is Required for Induction of Type 1 Immunity in a Mouse Model of Subcutaneous Infection by *Trypanosoma cruzi*. *J. Immunol.* **2006**, *177*, 6325–6735.

(12) Andrade, D.; Serra, R.; Svensjö, E.; Lima, A. P.; Ramos-Jr, E. S.; Fortes, F. S.; Morandini, A. C.; Morandi, V.; Soeiro, M. N.; Tanowitz, H. B.; Scharfstein, J. *Trypanosoma cruzi* Invades Host Cells Through the Activation of Endothelin and Bradykinin Receptors: A Converging Pathway Leading to Chagasic Vasculopathy. *Br. J. Pharmacol.* **2012**, *165*, 1333–1347.

(13) Du, X.; Guo, C.; Hansell, E.; Doyle, P. S.; Caffrey, C. R.; Holler, T. P.; McKerrow, J. H.; Cohen, F. E. Synthesis and Structure–Activity Relationship Study of Potent Trypanocidal Thio Semicarbazone Inhibitors of the Trypanosomal Cysteine Protease Cruzain. *J. Med. Chem.* **2002**, *45*, 2695–2707.

(14) Chiyanzu, I.; Hansell, E.; Gut, J.; Rosenthal, P. J.; McKerrow, J. H.; Chibale, K. Synthesis and Evaluation of Isatins and Thiosemicarbazone Derivatives Against Cruzain, Falcipain-2 and Rhodesain. *Bioorg. Med. Chem. Lett.* **2003**, *13*, 3527–3530.

(15) Greenbaum, D. C.; Mackey, Z.; Hansell, E.; Doyle, P.; Gut, J.; Caffrey, C. R.; Lehrman, J.; Rosenthal, P. J.; McKerrow, J. H.; Chibale, K. Synthesis and Structure–Activity Relationships of Parasiticidal Thiosemicarbazone Cysteine Protease Inhibitors against *Plasmodium falciparum*, *Trypanosoma brucei*, and *Trypanosoma cruzi*. *J. Med. Chem.* **2004**, *47*, 3212–3219.

(16) Fujii, N.; Mallari, J. P.; Hansell, E. J.; Mackey, Z.; Doyle, P.; Zhou, Y. M.; Gut, J.; Rosenthal, P. J.; McKerrow, J. H.; Guy, R. K. Discovery of Potent Thiosemicarbazone Inhibitors of Rhodesain and Cruzain. *Bioorg. Med. Chem. Lett.* **2005**, *15*, 121–123.

(17) Siles, R.; Chen, S. E.; Zhou, M.; Pinney, K. G.; Trawick, M. L. Design, Synthesis, and Biochemical Evaluation of Novel Cruzain

Inhibitors with Potential Application in the Treatment of Chagas Disease. *Bioorg. Med. Chem. Lett.* **2006**, *16*, 4405–4409.

(18) Porcal, W.; Hernández, P.; Boiani, M.; Aguirre, G.; Boiani, L.; Chidichimo, A.; Cazzulo, J. J.; Campillo, N. E.; Paez, J. A.; Castro, A.; Krauth-Siegel, R. L.; Davies, C.; Basombrio, M. A.; González, M.; Cerecetto, H. In Vivo Anti-Chagas Vinylthio-, Vinylsulfinyl-, and Vinylsulfonylbenzofuroxan Derivatives. *J. Med. Chem.* **2007**, *50*, 6004–6015.

(19) Guido, R. V.; Trossini, G. H.; Castilho, M. S.; Oliva, G.; Ferreira, E. I.; Andricopulo, A. D. Structure-Activity Relationships for a Class of Selective Inhibitors of the Major Cysteine Protease from *Trypanosoma cruzi*. *J. Enzyme Inhib. Med. Chem.* **2008**, *23*, 964–973.

(20) Pizzo, C.; Faral-Tello, P.; Salinas, G.; Flo, M.; Robello, C.; Wipf, P.; Mahler, S. G. Selenosemicarbazones as Potent Cruzipain Inhibitors and Their Antiparasitic Properties against *Trypanosoma cruzi*. *Med. Chem. Commun.* **2012**, *3*, 362–368.

(21) Merlino, A.; Benitez, M.; Campillo, N. E.; Páez, J. A.; Tinoco, L. W.; González, M.; Cerecetto, H. Amidines Bearing Benzofuroxan or Benzimidazole 1,3-Dioxide Core Scaffolds as *Trypanosoma cruzi*-Inhibitors: Structural Basis for Their Interactions with Cruzipain. *Med. Chem. Commun.* **2012**, *3*, 90–101.

(22) Brak, K.; Doyle, P. S.; McKerrow, J. H.; Ellman, J. A. Identification of a New Class of Nonpeptidic Inhibitors of Cruzain. *J. Am. Chem. Soc.* **2008**, *130*, 6404–6410.

(23) Brak, K.; Kerr, I. D.; Barrett, K. T.; Fuchi, N.; Debnath, M.; Ang, K.; Engel, J. C.; McKerrow, J. H.; Doyle, P. S.; Brinen, L. S.; Ellman, J. A. Nonpeptidic Tetrafluorophenoxymethyl Ketone Cruzain Inhibitors as Promising New Leads for Chagas Disease Chemotherapy. *J. Med. Chem.* **2010**, *53*, 1763–1773.

(24) Bryant, C.; Kerr, I. D.; Debnath, M.; Ang, K. K.; Ratnam, J.; Ferreira, R. S.; Jaishankar, P.; Zhao, D.; Arkin, M. R.; McKerrow, J. H.; Brinen, L. S.; Renslo, A. R. Novel Non-Peptidic Vinylsulfones Targeting the S2 and S3 Subsites of Parasite Cysteine Proteases. *Bioorg. Med. Chem. Lett.* **2009**, *19*, 6218–6221.

(25) Leite, A. C. L.; de Lima, R. S.; Moreira, D. R.; Cardoso, M. V. O.; Gouveia, A. C.; Santos, L. M.; Hernandes, M. Z.; Kiperstok, A. C.; de Lima, R. S.; Soares, M. B. P. Synthesis, Docking, and *In Vitro* Activity of Thiosemicarbazones, Aminoacyl-Thiosemicarbazides and Acyl-Thiazolidones Against *Trypanosoma cruzi*. *Bioorg. Med. Chem.* **2006**, *14*, 3749–3457.

(26) Leite, A. C.; Moreira, D. R.; Cardoso, M. V. O.; Hernandes, M. Z.; Pereira, V. R. A.; Silva, R. O.; Kiperstok, A. C.; Lima, M. S.; Soares, M. B. P. Synthesis, Cruzain Docking, and *In Vitro* Studies of Aryl-4-oxothiazolylhydrazones Against *Trypanosoma cruzi*. *ChemMedChem* **2007**, *2*, 1339–1345.

(27) Hernandes, M. Z.; Rabello, M. M.; Leite, A. C. L.; Cardoso, M. V. O.; Moreira, D. R. M.; Brondani, D. J.; Simone, C. A.; Reis, L. C.; Souza, M. A.; Pereira, V. R.; Ferreira, R. S.; McKerrow, J. H. Studies Toward the Structural Optimization of Novel Thiazolylhydrazone-Based Potent Antitrypanosomal Agents. *Bioorg. Med. Chem.* **2010**, *18*, 7826–7835.

(28) Lima, L. M.; Barreiro, E. J. Bioisosterism: a Useful Strategy for Molecular Modification and Drug Design. *Curr. Med. Chem.* **2005**, *23*–49.

(29) Zhang, D. N.; Li, J. T.; Song, Y. L.; Liu, H. M.; Li, H. Y. Efficient One-Pot Three-Component Synthesis of N-(4-arylthiazol-2-yl)-hydrazones in Water Under Ultrasound Irradiation. *Ultrason. Sonochem.* **2012**, *19*, 475–478.

(30) Chimenti, F.; Bizzarri, B.; Maccioni, E.; Secci, D.; Bolasco, A.; Chimenti, P.; Fioravanti, R.; Granese, A.; Carradori, S.; Tosi, F.; Ballario, P.; Vernarecci, S.; Filetici, P. A Novel Histone Acetyltransferase Inhibitor Modulating Gcn5 Network: Cyclopentylidene-[4-(4'-chlorophenyl)thiazol-2-yl]hydrazone. *J. Med. Chem.* **2009**, *52*, 530–536.

(31) Ferreira, R. S.; Bryant, C.; Ang, K. K.; McKerrow, J. H.; Shoichet, B. K.; Renslo, A. R. Divergent Modes of Enzyme Inhibition in a Homologous Structure–Activity Series. *J. Med. Chem.* **2009**, *52*, 5005–5058.

(32) Hernandes, M. Z.; Cavalcanti, S. M.; Moreira, D. R. M.; de Azevedo, W. F., Jr.; Leite, A. C. L. Halogen Atoms in the Modern

Medicinal Chemistry: Hints for the Drug Design. *Curr. Drug Targets* **2010**, *11*, 303–314.

(33) Engel, J. C.; Doyle, P. S.; Palmer, P.; Hsieh, I.; Bainton, D. F.; McKerrow, J. H. Cysteine Protease Inhibitors Alter Golgi Complex Ultrastructure and Function in *Trypanosoma cruzi*. *J. Cell Sci.* **1998**, *111*, 597–606.

(34) Pizzo, C.; Saiz, C.; Talevi, A.; Gavernet, L.; Palestro, P.; Bellera, C.; Blanch, L. B.; Benítez, D.; Cazzulo, J. J.; Chidichimo, A.; Wipf, P.; Mahler, S. G. Synthesis of 2-Hydrazolyl-4-Thiazolidinones Based on Multicomponent Reactions and Biological Evaluation Against *Trypanosoma cruzi*. *Chem. Biol. Drug Des.* **2011**, *77*, 162–177.

(35) Matsuo, A. L.; Silva, L. S.; Torrecilhas, A. C.; Pascoalino, B. S.; Ramos, T. C.; Rodrigues, E. G.; Schenkman, S.; Caires, A. C.; Travassos, L. R. *In Vitro* and *In Vivo* Trypanocidal Effects of the Cyclopalladated Compound 7a, a Drug Candidate for Treatment of Chagas' Disease. *Antimicrob. Agents Chemother.* **2010**, *54*, 3318–3325.

(36) Romanha, A. J.; Castro, S. L.; Soeiro, M. N.; Lannes-Vieira, J.; Ribeiro, I.; Talvani, A.; Bourdin, B.; Blum, B.; Olivieri, B.; Zani, C.; Spadafora, C.; Chiari, E.; Chatelain, E.; Chaves, G.; Calzada, J. E.; Bustamante, J. M.; Freitas-Jr, L. H.; Romero, L. I.; Bahia, M. T.; Lotrowska, M.; Soares, M. B. P.; Andrade, S. G.; Armstrong, T.; Degraeve, W.; Andrade, Z. A. *In Vitro* and *In Vivo* Experimental Models for Drug Screening and Development for Chagas Disease. *Mem. Inst. Oswaldo Cruz* **2010**, *105*, 233–238.

(37) Wilson, H. R.; Revankar, G. R.; Tolman, R. L. *In Vitro* and *In Vivo* Activity of Certain Thiosemicarbazones against *Trypanosoma cruzi*. *J. Med. Chem.* **1974**, *17*, 760–761.

(38) Otero, L.; Vieites, M.; Boiani, L.; Denicola, A.; Rigol, C.; Opazo, L.; Olea-Azar, C.; Maya, J. D.; Morello, A.; Krauth-Siegel, R. L.; Piro, O. E.; Castellano, E.; González, M.; Gambino, D.; Cerecetto, H. Novel Antitrypanosomal Agents Based on Palladium Nitrofurlythiosemicarbazone Complexes: DNA and Redox Metabolism as Potential Therapeutic Targets. *J. Med. Chem.* **2006**, *49*, 3322–3331.

(39) Vieites, M.; Otero, L.; Santos, D.; Toloza, J.; Figueroa, R.; Norambuena, E.; Olea-Azar, C.; Aguirre, G.; Cerecetto, H.; González, M.; Morello, A.; Maya, J. D.; Garat, B.; Gambino, D. Platinum(II) Metal Complexes as Potential Anti-*Trypanosoma cruzi* Agents. *J. Inorg. Biochem.* **2008**, *102*, 1033–1043.

(40) Maia, P. I.; Fernandes, A. G.; Silva, J. J.; Andricopulo, A. D.; Lemos, S. S.; Lang, E. S.; Abram, U.; Deflon, V. M. Dithiocarbazate Complexes With the $[M(PPh_3)]^{2+}$ (M = Pd or Pt) Moiety Synthesis, Characterization and Anti-*Trypanosoma cruzi* Activity. *J. Inorg. Biochem.* **2010**, *104*, 1276–1282.

(41) Caputto, M. E.; Ciccarelli, A.; Frank, F.; Moglioni, A. G.; Moltrasio, G. Y.; Vega, D.; Lombardo, E.; Finkielstein, L. M. Synthesis and Biological Evaluation of Some Novel 1-Indanone Thiazolylhydrazone Derivatives as Anti-*Trypanosoma cruzi* Agents. *Eur. J. Med. Chem.* **2012**, *55*, 155–163.

(42) Suryadevara, P. K.; Olepu, S.; Lockman, J. W.; Ohkanda, J.; Karimi, M.; Verlinde, C. L.; Kraus, J. M.; Schoepe, J.; Van-Voorhis, W. C.; Hamilton, A. D.; Buckner, F. S.; Gelb, M. H. Structurally Simple Inhibitors of Lanosterol 14 α -Demethylase Are Efficacious In a Rodent Model of Acute Chagas Disease. *J. Med. Chem.* **2009**, *52*, 3703–3715.

(43) Andriani, G.; Chessler, A. D.; Courtemanche, G.; Burleigh, B. A.; Rodriguez, A. Activity *In Vivo* of Anti-*Trypanosoma cruzi* Compounds Selected From a High Throughput Screening. *Plos Negl. Trop. Dis.* **2011**, *5*, e1298.

(44) Keenan, M.; Abbott, M. J.; Alexander, P. W.; Armstrong, T.; Best, W. M.; Berven, B.; Botero, A.; Chaplin, J. H.; Charman, S. A.; Chatelain, E.; Geldern, T. W.; Kerfoot, M.; Khong, A.; Nguyen, T.; McManus, J. D.; Morizzi, J.; Ryan, E.; Scandale, I.; Thompson, R. A.; Wang, S. Z.; White, K. L. Analogues of Fenarimol Are Potent Inhibitors of *Trypanosoma cruzi* and Are Efficacious in a Murine Model of Chagas Disease. *J. Med. Chem.* **2012**, *55*, 4189–4204.

(45) Rocha, G. B.; Freire, R. O.; Simas, A. M.; Stewart, J. J. P. RM1: A Reparameterization of AM1 for H, C, N, O, P, S, F, Cl, Br, and I. *J. Comput. Chem.* **2006**, *27*, 1101–1111.

(46) Spartan '08 Tutorial and user's guide; Wavefunction: Irvine, CA, 2008. <http://www.wavefun.com/products/spartan.html>.

(47) *Gold software, version 5.1*, Cambridge Crystallographic Data Centre. <http://www.ccdc.cam.ac.uk>.

(48) Durrant, J. D.; Mccammon, J. A. BINANA: A Novel Algorithm for Ligand-Binding Characterization. *J. Mol. Graph. Model.* **2011**, *29*, 888–893.

(49) DeLano, W. L. *The PyMOL Molecular Graphics System*, DeLano Scientific, San Carlos, CA, 2002. <http://www.pymol.org>.